Since January 2020 Elsevier has created a COVID-19 resource centre with free information in English and Mandarin on the novel coronavirus COVID-19. The COVID-19 resource centre is hosted on Elsevier Connect, the company's public news and information website.

Microbial Risk Analysis 15 (2020) 100104

Contents lists available at ScienceDirect

Microbial Risk Analysis

journal homepage: www.elsevier.com/locate/mran

How virus size and attachment parameters affect the temperature sensitivity of virus binding to host cells: Predictions of a thermodynamic model for arboviruses and HIV

Paul Gale

Independent Scientist, 15 Weare Close, Portland, Dorset, DT5 1JP, United Kingdom

ARTICLE INFO

Keywords:
Temperature
Virus size
Entropy
Antivirals
Heat capacity

ABSTRACT

Virus binding to host cells involves specific interactions between viral (glyco)proteins (GP) and host cell surface receptors (Cr) (protein or sialic acid (SA)). The magnitude of the enthalpy of association changes with temperature according to the change in heat capacity (ΔC_p) on GP/Cr binding, being little affected for avian influenza virus (AIV) haemagglutinin (HA) binding to SA (ΔC_p = 0 kJ/mol/K) but greatly affected for HIV gp120 binding to CD4 receptor (ΔC_p = −5.0 kJ/mol/K). A thermodynamic model developed here predicts that values of ΔC_p from 0 to ~−2.0 kJ/mol/K have relatively little impact on the temperature sensitivity of the number of mosquito midgut cells with bound arbovirus, while intermediate values of ΔC_p of ~−3.0 kJ/mol/K give a peak binding at a temperature of ~20 °C as observed experimentally for Western equine encephalitis virus. More negative values of ΔC_p greatly decrease arbovirus binding at temperatures below ~20 °C. Thus to promote transmission at low temperatures, arboviruses may benefit from ΔC_p ~ 0 kJ/mol/K as for HA/SA and it is interesting that bluetongue virus binds to SA in midge midguts. Large negative values of ΔC_p as for HIV gp120:CD4 diminish binding at 37 °C. Of greater importance, however, is the decrease in entropy of the whole virus (ΔS_{a_immob}) on its immobilisation on the host cell surface. ΔS_{a_immob} presents a repulsive force which the enthalpy-driven GP/Cr interactions weakened at higher temperatures struggle to overcome. ΔS_{a_immob} is more negative (less favourable) for larger diameter viruses which therefore show diminished binding at higher temperatures than smaller viruses. It is proposed that small size phenotype through a less negative ΔS_{a_immob} is selected for viruses infecting warmer hosts thus explaining the observation that virion volume decreases with increasing host temperature from 0 °C to 40 °C in the case of dsDNA viruses. Compared to arboviruses which also infect warm-blooded vertebrates, HIV is large at 134 nm diameter and thus would have a large negative ΔS_{a_immob} which would diminish its binding at human body temperature. It is proposed that prior non-specific binding of HIV through attachment factors takes much of the entropy loss for ΔS_{a_immob} so enhancing subsequent specific gp120:CD4 binding at 37 °C. This is consistent with the observation that HIV attachment factors are not essential but augment infection. Antiviral therapies should focus on increasing virion size, for example through

Abbreviations: AIV, avian influenza virus; BBF, brush border fragments from midgut; BTV, bluetongue virus; C_p, heat capacity at constant pressure; ΔC_p, change in heat capacity; Cr, host cell receptor; CD4, host cell receptor for HIV; C_{total}, number of host cells which can bind virus in a given volume of host fluid (midgut or blood); $C.V_T$, number of host cells with bound virus at temperature T; DENV, Dengue virus; E_A, activation energy; EBOV, Zaire ebolavirus; EM, electron microscopy; Env, HIV gp120 trimer envelope protein which binds to a single CD4 molecule; F_{cT}, fraction of arthropod midgut cells with bound virus at temperature T; $\Delta G_{a\_virus\_T}$, change in Gibbs free energy on association of virus and host cell at temperature T; GP, viral (glyco)protein on virus surface that binds to Cr; HA, haemagglutinin; $\Delta H_{a\_receptor\_T}$, change in enthalpy for binding of virus GP to host Cr receptor at a temperature T; HIV, human immunodeficiency virus; HSV-2, herpes simplex virus type 2; $\Delta H_{a\_virus\_T}$, change in enthalpy for binding of virus to host cell at temperature T; $K_{a\_virus\_T}$, association constant for binding of virus to host cells at temperature T; $K_{d\_receptor\_T}$, dissociation constant for GP from Cr at temperature T; K_{d_virus}, dissociation constant for virus from host cell; M, molar (moles dm^{-3}); n, number of GP/Cr contacts made on virus binding to cell; $p_{transmissionT}$, probability of successful infection of the arthropod salivary glands after oral exposure at temperature T; $p_{completeT}$, probability given a virion has bound to the surface of a midgut cell that that midgut cell becomes infected and that its progeny viruses go on to infect the salivary gland so completing the arthropod infection process within the life time of the arthropod at temperature T; R, ideal gas constant; $\Delta S_{a\_receptor\_T}$, change in entropy for binding of virus GP to host Cr receptor; $\Delta S_{a\_virus\_T}$, change in entropy for binding of virus to host cell at temperature T; ΔS_{a_immob}, change in entropy on immobilization of whole virus to cell surface; $\Delta S_{a\_non\_specific}$, change in entropy on immobilization of virus to cell surface through non-specific binding; $\Delta S_{a\_specific}$, change in entropy on immobilization of virus to cell surface through specific GP/Cr-driven binding; SA, sialic acid; SIV, simian immunodeficiency virus; V_{free}, virus not bound to cells; V_{total}, virus challenge dose in volume of host fluid; WEEV, Western equine encephalitis virus; WNV, West Nile virus; ZnOT, zinc oxide tetrapod

E-mail address: paul@galleryofbirds.com.

https://doi.org/10.1016/j.mran.2020.100104
Received 29 December 2019; Received in revised form 5 March 2020; Accepted 6 March 2020
Available online 12 March 2020

binding of zinc oxide nanoparticles to herpes simplex virus, hence making ΔS_{a_immob} more negative, and thus reducing binding affinity at 37 °C.

1. Introduction

Some viruses infect hosts over a range of temperatures depending on the host species. Most notable are the arboviruses which may infect the arthropod vector over a range of ambient temperatures from ~15 °C to >30 °C (Mullens *et al.*, 2004), and then infect a vertebrate host at temperatures from 37 °C up to 44 °C in the case of West Nile virus (WNV) in infected American crows (*Corvus brachyrhynchos*) (Kinney *et al.*, 2006). Birds generally have higher body temperatures than mammals (Brault 2009) and the avian influenza virus (AIV) when jumping from birds to humans has to adapt to a temperature drop of 8 °C since the temperature in the human upper respiratory tract is ~33 °C compared to ~41 °C in the avian intestinal tract which is the site of replication of avian viruses (De Graaf and Fouchier, 2014). Bats have higher core body temperatures than primates (up to 42.1 °C for *Phyllostomus hastatus* which is an omnivorous bat from South America) when flying (O'Shea *et al.*, 2014). The core body temperature during flight of the insectivorous free-tailed bat (*Mops condylurus*) which may have been the origin of the 2013/15 severe *Zaire ebolavirus* (EBOV) outbreak in West Africa (Saez *et al.*, 2015) is 40.5 °C ± 1 °C (O'Shea *et al.*, 2014). Thus EBOV which infects a range of vertebrate species from bats to primates and deer may have to infect mammalian hosts over a range of temperatures. Similarly Nipah virus on jumping from fruit bats to pigs and humans (Daszak *et al.*, 2013) may experience a small fall in temperature. Furthermore, cross-species transmission of viruses to bats (and other mammals) from invertebrates may occur with more regularity than has been appreciated (Bennett *et al.*, 2018; Leendertz 2016), and Bennett *et al.* (2018) have suggested that arthropods may host many "bat-associated" viruses that have defied detection in bats themselves (e.g. EBOV). Depending on the ambient temperature, viruses in arthropods would experience a 9 °C to 15 °C temperature increase on being ingested by a bat at 41 °C (Gale 2017) and this could affect the binding affinity of the virus to its host cell depending on the thermodynamics of virus binding as is discussed here. In contrast other viruses only infect related host species, and in effect are maintained at similar temperatures. For example, simian immunodeficiency viruses (SIV) infect 36 different nonhuman primate species in sub-Saharan Africa and SIVs from chimpanzees (*Pan troglodytes*) have crossed species barriers on multiple occasions generating human immunodeficiency virus (HIV) types 1 and 2 (Sharp *et al.*, 2005). Thus the main source of temperature variation experienced by SIV and HIV would be the effect of the circadian rhythm and the slight rise in temperature due to infection of the host which gives a range of 36 °C to 38 °C in the case of Rhesus monkeys (Huitron-Resendiz et al., 2007).

Viruses bind to host cells through interactions between a virus surface (glyco)protein (GP) and a host cell receptor (Cr). The Cr molecule on the cell surface may be a protein as in the case of HIV (Myszka *et al.*, 2000), EBOV (Yuan *et al.*, 2015), Hendra virus (Xu *et al.*, 2012) and MERS-CoV (Lu *et al.*, 2013) or alternatively is a sialic acid (SA) on a glycan as in the case of AIV (De Graaf and Fouchier, 2014; Fei *et al.*, 2015) and arboviruses such as bluetongue virus (BTV) (Zhang *et al.*, 2010). The thermodynamics of virus binding in terms of the changes in enthalpy ($\Delta H_{a\_receptor\_T}$) and entropy ($\Delta S_{a\_receptor\_T}$) on the specific interaction of the GP with the Cr receptor at temperature T during binding of virus to the host cell surface has been set out previously (Gale 2018, 2019). The interactions between the HIV GP and its CD4 cellular receptor (Myszka *et al.*, 2000; Dey *et al.*, 2007) and between the AIV haemagglutinin (HA) and its α2,3-SA or α2,6-SA receptors (Fei *et al.*, 2015) are enthalpy driven, i.e. large negative values of $\Delta H_{a\_receptor\_T}$ overcome unfavourable values of $\Delta S_{a\_receptor\_T}$. Also the binding of vesicular stomatitis virus to phospholipid bilayers is enthalpy driven (Carneio *et al.* 2002) with very large negative values of $\Delta H_{a\_receptor\_T}$.

Temperature may impose constraints on viruses' jumping the species barrier through its effect on the binding affinity of GP to Cr. There may also be constraints on the activities of viral replication proteins such as the AIV polymerase which showed a significantly higher activity at 33 °C than 37 °C (Ngai *et al.*, 2013). Only virus binding is considered here. Thus according to the Van't Hoff Isochore, the binding affinity for a virus to its host cell at temperature T as represented by the association constant $K_{a\_virus\_T}$ would be greatly diminished for enthalpy-driven GP/Cr interactions at higher temperatures compared to lower temperatures depending on the magnitude of $\Delta H_{a\_receptor\_T}$ (Gale 2019). Indeed, assuming $\Delta H_{a\_receptor\_T}$ is constant over the temperature range, the more negative $\Delta H_{a\_receptor\_T}$ is in magnitude, the weaker the binding at higher temperatures. This presents a paradox if the $K_{a\_virus\_T}$ falls to less than $\sim 10^{14}$ M^{-1} in that higher temperatures would greatly diminish infectivity (Gale 2019).

While the values of $\Delta H_{a\_receptor\_T}$ and $\Delta S_{a\_receptor\_T}$ may be constant over the biological temperature range for some GP/Cr systems, e.g. AIV haemagglutinin (HA) binding to sialic acid (SA) residues (Fei *et al.*, 2015) they may change considerably in magnitude over the biologically relevant temperature range particularly for protein:protein systems as in the case of HIV gp120 binding to CD4 (Myszka *et al.*, 2000) (Fig. 1). The effect of this on $K_{a\_virus\_T}$ is considered in this work. The change in $\Delta H_{a\_receptor\_T}$ with temperature is defined by the difference in heat capacities (C_p) of the GP/Cr "product" complex and the free GP/free host Cr "reactants" and is represented by ΔC_p which is the slope of the lines in Fig. 1 and typically ranges from ~0 kJ/mol/K to −5.0 kJ/mol/K depending on the system.

The previous thermodynamic treatment of virus binding (Gale 2019) identified the entropy change (ΔS_{a_immob}) on immobilisation of the whole virus particle on the host cell surface as a key parameter for which there are currently no data. ΔS_{a_immob} would be expected to be large and negative in magnitude due to the decrease in the absolute entropy on immobilisation of a large molecular entity such as a virion. A recent analysis has shown that virion volume (and genome length) for dsDNA viruses decreases by about 55-fold as the temperature of occurrence (i.e. host) increases from 0 to 40 °C (Nifong and Gillooly 2016). The temperature of occurrence in these dsDNA viruses ranges from near zero for those inhabiting polar environments to over

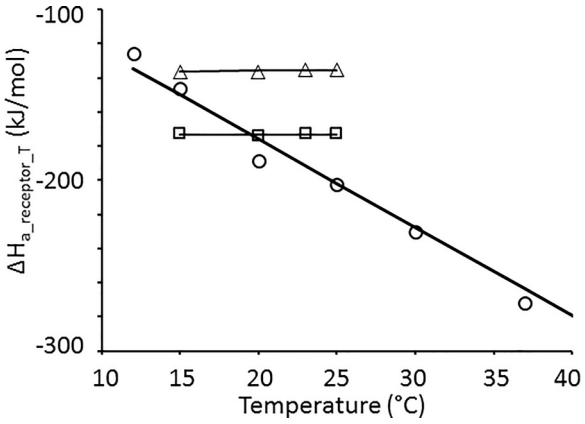

Fig. 1. Variation in $\Delta H_{a\_receptor\_T}$ as a function of temperature as reported for HIV gp120 monomer binding to CD4 (○) (Myszka *et al.*, 2000) and AIV HA monomer binding to soluble α2–6 sialyllactose (Δ) and α2–3 sialyllactose (□) (Fei *et al.*, 2015). The slopes of the lines represent the ΔC_p values which are summarised in Table 3.

40 °C for those inhabiting endothermic vertebrates. Nifong and Gillooly (2016) suggest that this could reflect smaller viruses being able to replicate more quickly (due to more compact genomes) perhaps together with energetic constraints imposed by their hosts. However from the thermodynamic perspective, the decrease in volume and hence mass and radius of the virus will make ΔS_{a_immob} less negative for a smaller virus than for a larger virus. It is shown here how a less negative ΔS_{a_immob} increases binding of the virus at the relatively high mammalian body temperatures and it is proposed that thermodynamic binding constraints may give smaller viruses a selective advantage for infecting hosts at the higher body temperatures of mammals and birds. In this respect, the large size of the HIV virion may present a constraint to binding at human body temperatures compared to the much smaller arboviruses for example.

In the case of HIV, the GP component of the GP/Cr interaction is the envelope protein (Env) which is a trimer of gp120 monomers. Each HIV Env trimer interacts with one CD4 molecule (Chuang *et al.*, 2017; Liu *et al.*, 2017a). This is different from the AIV HA trimer in which each monomer in the trimer interacts with one glycan Cr (De Graaf and Fouchier, 2014; Fei *et al.*, 2015). Initial attachment of the HIV virion to the host $CD4^+$ *T* cell surface is relatively nonspecific (Wilen *et al.*, 2012) with HIV Env interacting with negatively charged host cell surface heparan sulphate proteoglycans, or with pattern recognition receptors. According to Wilen *et al.* (2012), non-specific HIV attachment to the host cell via any of these factors likely brings HIV Env into close proximity with the viral receptor CD4 and the CRR5 coreceptor, so increasing the efficiency of infection, although the physiologic role of non-specific attachment in vivo remains unclear. Here it is suggested that non-specific binding helps to overcome the thermodynamic entropy constraint of immobilisation of a large virus on binding at human body temperature by taking some of the entropy loss in ΔS_{a_immob} prior to specific HIV Env:CD4 binding. This would be consistent with the fact that non-specific attachment factors differ from receptors in that they are not essential, although they augment infection in vitro (Wilen *et al.*, 2012).

A review of the literature has not found any results for the effect of temperature on the binding of HIV to $CD4^+$ *T* cells with which to test or validate the HIV thermodynamic binding model developed here. However, Frey *et al.* (1995) reported the binding of cells expressing HIV GP on their surface to $CD4^+$ *T* cells over the temperature range of 0 °C to 42 °C. It is known that increasing host membrane fluidity at higher temperature allows effective recruitment of more Cr molecules to bind the HIV virion (Harada *et al.*, 2004) such that the number, n, of GP/Cr contacts increases with temperature (Frey *et al.*, 1995), and that increasing n can overcome both the effect of temperature on decreasing the GP/Cr binding affinity and the effect of a large negative ΔS_{a_immob} (Gale 2019). The thermodynamic HIV binding model here is therefore modified to accommodate increasing n with temperature and so attempt to reproduce the results of Frey *et al.* (1995). The success of the model here is in predicting the subsequent decrease in binding reported by Frey *et al.* (1995) at higher temperatures due to ΔS_{a_immob}.

Here six case studies are presented to illustrate the effects of the magnitude of n, ΔC_p and ΔS_{a_immob} on the temperature sensitivity of virus binding. These are:-

1 The predicted effect of the magnitude of ΔC_p on the temperature dependence of Dengue virus (DENV) transmission by *Aedes albopictus*;
2 The predicted effect of the magnitude of ΔC_p on the temperature peak observed for the specific binding of Western equine encephalitis virus (WEEV) to susceptible *Culex tarsalis* brush border fragments (BBFs);
3 A large negative ΔC_p for a protein:protein GP/Cr system as represented by HIV gp120:CD4 diminishes host cell binding at human body temperature;
4 A large virus diameter as for the HIV virion diminishes host cell binding at the higher temperature of the human body through the large negative ΔS_{a_immob};
5 Non-specific attachment factors may partially overcome the unfavourable ΔS_{a_immob} and hence enhance specific HIV binding through Env:CD4 interactions at human body temperature; and
6 Increasing the number, n, of GP/Cr contacts with temperature to reproduce the data of Frey *et al.* (1995) for binding of HIV Env-expressing cells to cells expressing CD4.

Table 1
Equations used. See methods for derivation.

$$H_T = H_{T_0} + C_p(T - T_0) \quad \text{(Eq. 1)}$$

$$\mathrm{GP} + \mathrm{Cr} \leftrightarrow \mathrm{GP.Cr} \quad \text{(Eq. 2)}$$

$$\Delta H_{a\_receptor\_T} = H_T(GP{\cdot}Cr) - (H_T(GP) + H_T(Cr)) \quad \text{(Eq. 3)}$$

$$\Delta H_{a\_receptor\_T} = \Delta H_{a\_receptor\_T_0} + \Delta C_p(T - T_0) \quad \text{(Eq. 4)}$$

$$\Delta C_p = C_p(GP{\cdot}Cr) - (C_p(GP) + C_p(Cr)) \quad \text{(Eq. 5)}$$

$$\Delta S_{a\_receptor\_T} = \Delta S_{a\_receptor\_T_0} + \Delta C_p ln\frac{T}{T_0} \quad \text{(Eq. 6)}$$

$$\Delta \mathrm{H}_{a\_virus\_T} = n \times \Delta \mathrm{H}_{a\_receptor\_T} \quad \text{(Eq. 7)}$$

$$\Delta \mathrm{S}_{a\_virus\_T} = \Delta \mathrm{S}_{a\_immob} + n \times \Delta \mathrm{S}_{a\_receptor\_T} \quad \text{(Eq. 8)}$$

$$\Delta \mathrm{G}_{a\_virus\_T} = \Delta \mathrm{H}_{a\_virus\_T} - T\Delta \mathrm{S}_{a\_virus\_T} \quad \text{(Eq. 9)}$$

$$\Delta G_{a\_virus\_T} = n\Delta H_{a\_receptor\_T} - nT\Delta S_{a_{receptor\_T}} - T\Delta S_{a\_immob} \quad \text{(Eq. 10)}$$

$$\Delta G_{a\_virus\_T} = n\Delta H_{a\_receptor\_T_0} - nT\Delta S_{a\_receptor\_T_0} + n\Delta C_p\left(T - T_0 - Tln\frac{T}{T_0}\right) - T\Delta S_{a\_immob} \quad \text{(Eq. 11)}$$

$$K_{a\_virus\_T} = exp\left(\frac{-\Delta G_{a\_virus\_T}}{RT}\right) \quad \text{(Eq. 12)}$$

$$F_{cT} = \frac{[V_{free}]}{[V_{free}] + 1/K_{a\_virus\_T}} \quad \text{(Eq. 13)}$$

$$C.\ V_T = F_{cT} \times C_{total} \quad \text{(Eq. 14)}$$

$$p_{completeT} = p_{complete283} \times e^{\left(\frac{E_A}{R}\times\left(\frac{1}{283} - \frac{1}{T}\right)\right)} \quad \text{(Eq. 15)}$$

$$p_{transmissionT} = 1 - (1 - p_{completeT})^{C.V_T} \quad \text{(Eq. 16)}$$

$$K_{a\_virus\_T} = \frac{1}{(K_{d\_receptor\_T})^n} \times e^{\frac{\Delta S_{a\_immob}}{R}} \quad \text{(Eq. 17)}$$

$$\Delta S_{a\_immob} \propto -ln\left(\frac{4}{3}\pi r^3\right) - 3ln\left(\left(\frac{4}{3}\pi r^3\right)r^2\right) \quad \text{(Eq. 18)}$$

$$\Delta S_{a\_specific} = \Delta S_{a\_immob} - \Delta S_{a\_non\_specific} \quad \text{(Eq. 19)}$$

It may be thought there is little point in modelling HIV binding with temperature because HIV only infects human hosts at ~37 °C. However, the model here suggests mammalian temperature may be a constraint on HIV binding (due to the large negative ΔC_p and ΔS_{a_immob}) in effect exposing a potential weakness in the HIV infection process which could be exploited for antiviral therapy. The implications of making ΔS_{a_immob}

more negative are considered here as a novel approach to developing antiviral therapies with reference to Antoine *et al.* (2012) using zinc oxide nanoparticles for preventing infection by herpes simplex virus type 2 (HSV-2).

2. Methods

2.1. The change in heat capacity (ΔC_p) on binding of virus GP to Cr receptors on the host cell

The change in enthalpy (H) with temperature (T) at constant pressure is the heat capacity, C_p.

$$\left(\frac{\partial H}{\partial T}\right)_p = C_p$$

Integrating with respect to temperature relates the absolute enthalpy (H_T) at temperature T to that (H_{T0}) at a given reference temperature T_0 through C_p according to Eq. (1) (see Table 1). The attachment of a virus to its host cell is driven by the n individual interactions between GP and Cr made on binding as represented by the dynamic equilibrium in Eq. (2). The change in enthalpy for GP binding to Cr at temperature T, $\Delta H_{a\_receptor\_T}$, is given by Eq. (3).

Substituting Eq. (1) into Eq. (3) for the enthalpies for the GP.Cr complex (H_T(GP.Cr)), the free GP (H_T(GP)) and the free Cr (H_T(Cr)) relates the enthalpy change for GP binding to Cr at temperature T, $\Delta H_{a\_receptor\_T}$, to that ($\Delta H_{a\_receptor\_T0}$) measured experimentally at temperature T_0 (Du *et al.*, 2016) according to Eq. (4) where ΔC_p is the change in heat capacity defined as the difference between the heat capacities of the GP.Cr complex and the sum of the heat capacities of the free GP and Cr molecules as given by Eq. (5). Similarly the entropy change ($\Delta S_{a\_receptor\_T}$) for GP binding to Cr at temperature T is related to that ($\Delta S_{a\_receptor\_T0}$) measured experimentally at temperature T_0 (Du *et al.*, 2016) according to Eq. (6).

2.2. Modelling the effect of temperature on $\Delta H_{a\_virus\_T}$ and $\Delta S_{a\_virus\_T}$ and hence $K_{a\_virus\_T}$

$\Delta H_{a\_virus\_T}$ and $\Delta S_{a\_virus\_T}$ are the changes in enthalpy and entropy respectively on binding of virus to host cell at temperature T. Substituting the terms for $\Delta H_{a\_virus\_T}$ (Eq. (7)) and $\Delta S_{a\_virus\_T}$ (Eq. (8)) into Eq. (9) expresses $\Delta G_{a\_virus\_T}$ in terms of n, ΔS_{a_immob}, $\Delta H_{a\_receptor\_T}$ and $\Delta S_{a\_receptor\_T}$ (Eq. (10)) where $\Delta G_{a\_virus\_T}$ is the change in Gibbs free energy on association of virus with a host cell at temperature T and ΔS_{a_immob} is the change in entropy on immobilisation of the whole virus on the cell surface (Gale 2018; 2019).

2.2.1. The change in heat capacity on virus binding to its host cell

For this work it is assumed that the change in heat capacity on binding of a virus to a host cell is determined by the change in heat capacity on interaction of GP with Cr according to Eq. (5) and that ΔS_{a_immob} in Eq. (10) is unaffected. In effect therefore the heat capacity of the "bulk" (i.e. non-GP/Cr) of the bound virus/host cell is the same as the sum of the heat capacities for the free virus and free host cell. This is acceptable because a change in heat capacity is related to a change in conformation of the molecular components (Myszka *et al.*, 2000) and the conformation of the bulk of the host cell and the virus would be unaffected by attachment. Indeed, ΔS_{a_immob} is mainly related to changes in rotational and translational mobility of the virus particle as a whole (see below) and does not involve the conformational changes in GP and Cr which are accommodated in the $\Delta S_{a\_receptor\_T}$ term (Gale 2019). Since the heat capacity of the "bulk" of the bound virus/host cell is the same as the sum of the heat capacities for the free virus and free host cell, ΔC_p for the bulk equals zero, and according to Eq. (6) therefore, ΔS_{a_immob} itself at temperature T (calculated as $\Delta S_{a\_immob\_T} = \Delta S_{a\_immob\_T0} + \Delta C_p.\ln(T/T_0)$) would be unaffected by temperature and hence constant as assumed in the models here.

2.2.2. The effect of the magnitude of ΔC_p on virus binding affinity at temperature T

Substituting $\Delta H_{a\_receptor\_T}$ and $\Delta S_{a\_receptor\_T}$ from Eqs. (4) and (6) respectively into Eq. (10) gives Eq. (11) from which $K_{a\_virus\_T}$ is calculated according to Eq. (12) where R is the ideal gas constant.

2.2.3. The choice of reference temperature, T_0

Comparing the predicted effect on $K_{a\_virus\_T}$ of the magnitude of ΔC_p in Case studies 1, 2 and 3 requires a reference temperature, T_0, to be defined at which the plots of $K_{a\_virus\_T}$ intercept. Values of $K_{a\_virus\_T}$ intercept at $T = T_0$ because the $n.\Delta C_p$ ($T - T_0 + T.\ln(T/T_0)$) term in Eq. (11) equals zero. Therefore for the purpose of demonstrating the effect of ΔC_p on the temperature sensitivity of $K_{a\_virus\_T}$, T_0 needs to be chosen to be well above or below the temperature range of interest. It should be noted that the choice of reference temperature is artificial and is only used here out of necessity to demonstrate the effect of different ΔC_p values while fixing the $K_{a\_virus\_T}$ intercept temperature. Indeed a given GP/Cr system has its own natural ΔC_p value which cannot be altered and is measured experimentally (Myszka *et al.*, 2000; Fei *et al.*, 2015). The T_0 temperature of 37 °C is appropriate to study arthropod vector competence for arbovirus transmission over the 10 to 35 °C temperature range in Case studies 1 and 2 as used previously for the arthropod vector competence model (Gale 2019). However, since 37 °C is the human body temperature at which HIV binds to host cells, 37 °C is not a good choice for T_0 in case study 3 for which T_0 is therefore set to 4 °C. The reference temperature is 37 °C in Case studies 4, 5 and 6 because the experimentally measured value of ΔC_p for HIV gp120:CD4 binding (Fig. 1) is used together with $\Delta H_{a\_receptor\_T0}$ and $\Delta S_{a\_receptor\_T0}$ values measured experimentally at a temperature T_0 of 37 °C (Myszka *et al.*, 2000), i.e. real data are used.

2.3. Case study 1: The predicted effect of the magnitude of ΔC_p on the temperature dependence of DENV transmission by Aedes albopictus

The approach for modelling arbovirus transmission efficiency by the arthropod vector has been fully described previously (Gale 2019) and is summarised here for the purpose of the models in Figs. 2 and 3.

2.3.1. Modelling $K_{a\_virus\_T}$ as a function of temperature

The strength of GP/Cr binding at temperature T is often expressed as the dissociation constant, $K_{d\_receptor\_T}$, for which smaller values indicate stronger binding (Xiong *et al.*, 2013). The thermodynamic model is based on an enthalpy-driven GP/Cr interaction with a $K_{d\_receptor\_T0}$ of 10^{-3} M at 37 °C (T_0) as used previously (Gale 2019) to represent the interaction between an arbovirus GP and a SA glycan (Cr) on the brush border surface of the epithelial cells lining the arthropod midgut. The parameters $\Delta H_{a\_receptor\_T0}$ and $\Delta S_{a\_receptor\_T0}$ at $T_0 = 37$ °C for DENV transmission by *Aedes albopictus* together with n and ΔS_{a_immob} are set out in Table 2 and values of $K_{a\_virus\_T}$ over the temperature range 10–37 °C are calculated for the ΔC_p values in Table 3 using $\Delta G_{a\_virus\_T}$ from Eq. (11) in Eq. (12).

2.3.2. Modelling the effect of temperature on the number of cells in the arthropod midgut with bound arbovirus

The arbovirus challenge dose is 10^5 virions and the midgut volume is 10^{-6} dm^3 giving a virus concentration $[V_{total}] = 1.7 \times 10^{-13}$ M. The fraction (F_{cT}) of arthropod midgut cells with bound arbovirus at temperature T is calculated from $K_{a\_virus\_T}$ using Eq. (13) assuming the concentration of free virus ($[V_{free}]$) ~ $[V_{total}]$. The number, $C.V_T$, of midgut cells with bound arbovirus at temperature T is calculated by multiplying F_{cT} by the total number of midgut cells ($C_{total} = 1000$) (Eq. (14)) as described previously (Gale 2019).

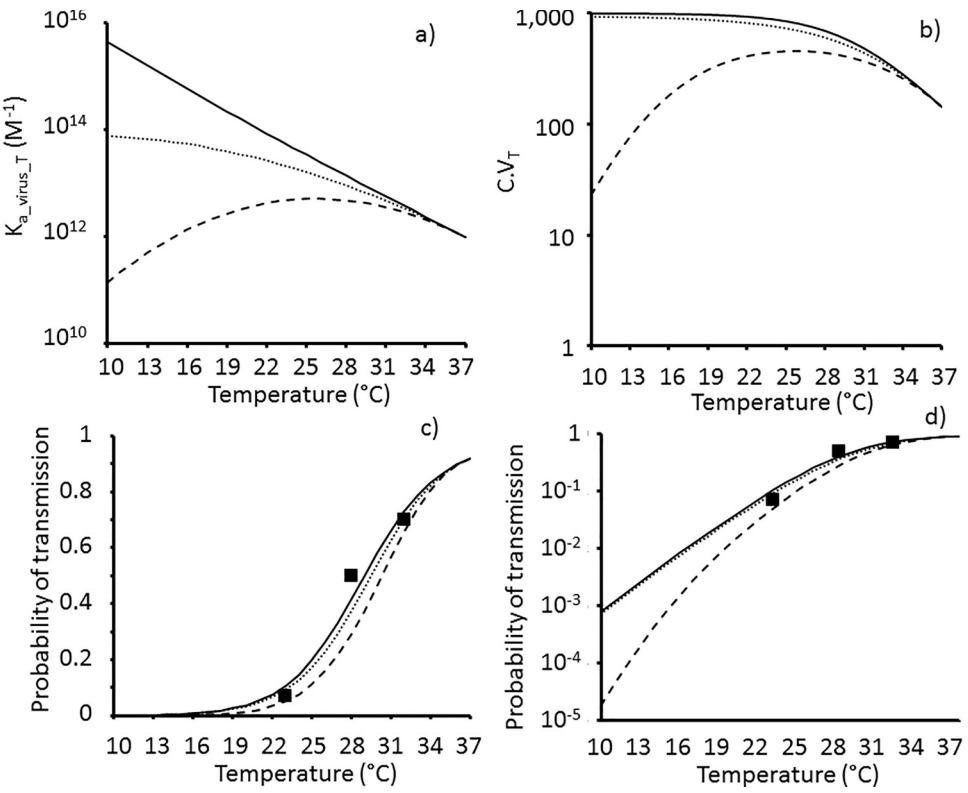

Fig. 2. Temperature variation of a) $K_{a\_virus\_T}$; b) C.V_T, c) and d) $p_{transmissionT}$ for ΔC_p = 0 (solid line), −1.97 (dotted line) and −5.02 (dashed line) kJ/mol/K (Table 3) with model parameters for arbovirus binding to mosquito midgut cells in Table 2 and ΔS_{a_immob} = 0 J/mol/K. Experimental data (■) in c) and d) for DENV transmission efficiency by *Aedes albopictus* mosquitoes from Liu *et al.* (2017b).

2.3.3. Modelling the effect of temperature on the arbovirus transmission efficiency

The probability, $p_{completeT}$, of an arthropod midgut cell with bound virus successfully leading to infection of the arthropod salivary glands and completion of virogenesis within in the lifetime of the arthropod at temperature T is calculated using the Arrhenius equation (Eq. (15)) where $p_{complete283}$ is the probability of this happening at 10 °C (283 K) and E_A is the activation energy of the rate-limiting step in virogenesis (Table 2). The probability, $p_{transmissionT}$, of arbovirus transmission by the arthropod (i.e. successful infection of the arthropod salivary glands after oral exposure) at temperature T given C.V_T midgut cells have bound virus is given by Eq. (16).

2.4. Case study 2: The magnitude of ΔC_p could explain the temperature peak observed in the specific binding of WEEV to susceptible Culex tarsalis BBFs

The value of ΔC_p in Eq. (11) with the GP/Cr binding parameters for DENV in Table 2 was optimised so that C.V_T as a function of temperature best approximated the specific binding affinity of WEEV to BBFs from susceptible *Culex tarsalis* mosquitoes as determined by Houk *et al.* (1990) and shown in Fig. 3.

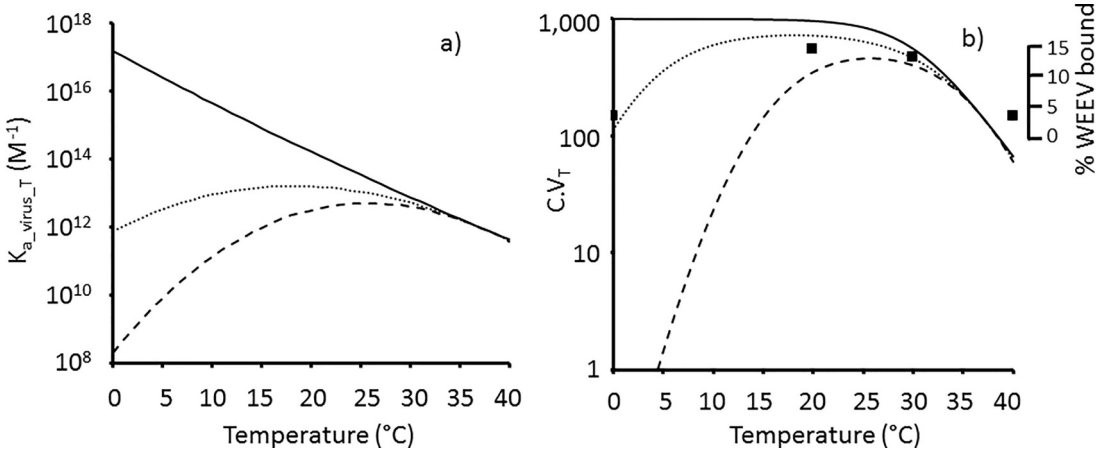

Fig. 3. Temperature variation of a) $K_{a\_virus\_T}$ and b) C.V_T for ΔC_p = 0 (solid line), −3.0 (dotted line) and −5.02 (dashed line) kJ/mol/K (Table 3) with model parameters for arbovirus binding to mosquito midgut cells in Table 2 and ΔS_{a_immob} = 0 J/mol/K. Experimental data (■) in b) show specific binding (as the percentage of total virus bound) of Western equine encephalitis virus (WEEV) to brush border fragments from susceptible *Culex tarsalis* mosquitoes as determined by Houk *et al.* (1990).

Table 2
Summary of the parameters for the enthalpy-driven GP/Cr binding model for DENV transmission by *Aedes albopictus* developed previously (Gale 2019).

Parameter	Value
Replication kinetic parameters for Eq. (15)	
$p_{complete283}$ (10 °C)	8.0×10^{-7}
E_A (kJ/mol)	270.0
GP/Cr binding parameters	
$\Delta H_{a\_receptor\_T0}$ at 37 °C (kJ/mol)	−56.545
$\Delta S_{a\_receptor\_T0}$ at 37 °C (J/mol/K)	−125
$K_{d\_receptor\_T0}$ at 37 °C	10^{-3} M
Whole virus binding parameters	
ΔS_{a_immob} (J/mol/K)	0
Number of GP/Cr contacts (n)	4
$\Delta H_{a\_virus\_T0}$ (kJ/mol) from Eq. (7)	−226.2
$\Delta S_{a\_virus\_T0}$ (J/mol/K) from Eq. (8)	−500

2.5. Case study 3: A large negative ΔC_p for a protein:protein GP/Cr system as represented by HIV gp120:CD4 diminishes host cell binding at higher temperatures

2.5.1. Estimation of n for HIV

Yang *et al.* (2005) using defective HIV gp120 monomers concluded that a single Env trimer is sufficient to mediate the entry of one virion, but that all three gp120 monomers in that trimer must be active. Klasse (2012) has proposed that a realistic model allows both a minimum requirement of two gp120 monomers with an increment in function by the third. This is consistent with the cryo-electron microscopy (EM) structure of the Env glycoprotein trimer (Liu *et al.*, 2017a) showing that in each trimer, one gp120 monomer makes a primary contact with the bound CD4 Cr molecule while a second makes a partial contact (called the quaternary contact reflecting protein structure nomenclature) and the third gp120 monomer makes no direct contact with the CD4 at all. For the purpose of the model here, n represents the number of Env trimers on each HIV virion that interact with a CD4 Cr during binding. Brandenberg *et al.* (2015) demonstrate that divergent HIV strains differ in their stoichiometry of entry and require between 1 and 7 Env trimers, with most strains depending on 2 to 3 Env trimers to complete infection. Here it is assumed that $n = 3$ Env:CD4 interactions for HIV binding although the results of Brandenberg *et al.* (2015) do not separate cell surface binding itself from the subsequent HIV/cell fusion in the entry process. If it is later found that cell surface binding only requires one Env:CD4 interaction for example, while more are required for the membrane fusion, then the model here for $C.V_T$ should be re-parameterised with $n = 1$ although the number of Env:CCR5 and non-specific Env interactions with attachment factors (see below) should also be built into the model. It should be noted that as for the arbovirus model, it is assumed that the $n = 3$ Env:CD4 interactions act independently and not co-operatively in binding. This is reflected in Eqs. (7) and (8) where $\Delta H_{a\_receptor\_T}$ and $\Delta S_{a\_receptor\_T}$ act additively.

2.5.2. Thermodynamic parameters for HIV Env:CD4 binding at T_0 of 37 °C

The Env trimer binds a single soluble CD4 with a $K_{d\_receptor\_T}$ (25 °C) of 1.4×10^{-9} M (Chuang *et al.*, 2017) which is 15-fold higher than that for the gp120 monomer:CD4 interaction estimated at 25 °C from the data of Myszka *et al.* (2000) in Table 4. To the author's knowledge there are no data for $\Delta H_{a\_receptor\_T}$ and $\Delta S_{a\_receptor\_T}$ for Env trimer binding to CD4. Therefore the values for $\Delta H_{a\_receptor\_T0}$ and $\Delta S_{a\_receptor\_T0}$ for HIV gp120 monomer:CD4 binding at 37 °C from Myszka *et al.* (2000) are used for Env trimer binding to a single CD4 in the HIV model in Fig. 4a and b as set out in Table 4. Dey *et al.* (2007) reported values at 37 °C of −287.9 kJ/mol and –786.9 J/mol/K for $\Delta H_{a\_receptor\_T}$ and $\Delta S_{a\_receptor\_T}$ respectively for the wildtype HIV-1 YU2 gp120 monomer binding to soluble CD4. The more negative $\Delta S_{a\_receptor\_T}$ value for gp120 monomer:CD4 binding from Dey *et al.* (2007) reduces the binding affinity for gp120:CD4 by nine-fold ($K_{d\_receptor\_T} = 4.2 \times 10^{-8}$ M) at 37 °C compared to that of 4.75×10^{-9} M from Myszka *et al.* (2000) (Table 4). This difference may simply reflect the different strains of HIV-1 used, namely YU2 by Dey *et al.* (2007) and WD61 by Myszka *et al.* (2000). The HIV gp120 monomer:CD4 binding data of Myszka *et al.* (2000) are chosen here over those of Dey *et al.* (2007) because Myszka *et al.* (2000) present the variation in $\Delta H_{a\_receptor\_T}$ with temperature as shown in Fig. 1 together with information on ΔC_p which Dey *et al.* (2007) do not consider. It is therefore assumed here that $\Delta C_p = -5.02$ kJ/mol/K for the Env trimer:CD4 interaction as reported by Myszka *et al.* (2000) for the gp120 monomer:CD4 interaction (Table 3).

Values of $\Delta S_{a\_receptor\_T}$ are not documented by Myszka *et al.* (2000) other than that at 37 °C (Table 4) and values at lower temperatures are therefore calculated from that at $T_0 = 37$ °C according to Eq. (6) using $\Delta C_p = -5.02$ kJ/mol/K for HIV gp120:CD4 (Table 3). Some reassurance that Eq. (6) is appropriate is that the value of $\Delta S_{a\_receptor\_T}$ of −493 J/mol/K predicted at $T = 25$ °C by Eq. (6) is very close to that of −473 J/mol/K calculated from the –T. $\Delta S_{a\_receptor\_T}$ value reported by

Table 4
Thermodynamic parameters for HIV Env binding to CD4 receptor at different temperatures. In the absence of data, the binding parameters for HIV Env trimer to CD4 as used in the models here are based on those from Myszka *et al.* (2000) for the full-length gp120 monomer binding to CD4.

	37 °C	4 °C	25 °C
$\Delta H_{a\_receptor\_T}$ (kJ/mol)	−263.59[a]	−97.9[c]	−198.2[e]
$\Delta S_{a\_receptor\_T}$ (J/mol/K)	−691.04[b]	−126.01[d]	−472.9[e,f]
$K_{d\_receptor\_T}$ (M)	4.75×10^{-9}	1.28×10^{-12}	[e]0.91×10^{-10}

[a] From Myszka *et al.* (2000) for full length gp120 (reported as −63 kcal/mol) at 37 °C.
[b] Calculated from $-T\Delta S = +214.22$ kJ/mol for full length gp120 (reported as +51.2 kcal/mol by Myszka *et al.* (2000)) at 37°C.
[c] Calculated from Eq. (4) using $\Delta C_p = -5.02$ kJ/mol/K (Table 3) with $T_0 = 310$ K (37 °C).
[d] Calculated from Eq. (6) using $\Delta C_p = -5.02$ kJ/mol/K (Table 3) with $T_0 = 310$ K (37 °C).
[e] Estimated from values for $\Delta H_{a\_receptor\_T}$ and $-T\Delta S_{a\_receptor\_T}$ presented in Fig. 4 of Myszka *et al.* (2000) for gp120 binding to CD4 at 25 °C.
[f] In good agreement with $\Delta S_{a\_receptor\_T}$ value at $T = 298$ K (25 °C) of −492.8 J/mol/K as calculated from Eq. (6) using $\Delta C_p = -5.02$ kJ/mol/K (Table 3) with $T_0 = 310$ K (37 °C) and $\Delta S_{a\_receptor\_T0} = -691.04$ J/mol/K (see b).

Table 3
Summary of some published ΔC_p values for protein/protein and protein/sialic acid (SA) interactions.

System	$K_{d\_receptor\_T}$ (Temperature)	ΔC_p kJ/mol/K (95% c.i.)	Temperature range of experiment	References
HIV gp120 monomer: CD4	5×10^{-9} M (37 °C)	−5.02 (± 0.84)	12 to 44 °C	Myszka *et al.* (2000)
E3 in pyruvate dehydrogenase multienzyme complex	6×10^{-10} M (25 °C)	−1.32 (±0.06)	10 to 37 °C	Jung *et al.* (2002)
E1 in pyruvate dehydrogenase multienzyme complex	3×10^{-10} M (25 °C)	−1.97 (±0.06)	10 to 37 °C	Jung *et al.* (2002)
AIV HA monomer: SAα−2,6	4.8×10^{-2} M (25 °C)	+0.125*	15 to 25 °C	Fei *et al.* (2015)
AIV HA monomer: SAα−2,3	2.6×10^{-2} M (25 °C)	−0.0074*	15 to 25 °C	Fei *et al.* (2015)

* Analysis of the data of Fei *et al.* (2015) by using their reported $\Delta G/T\Delta S$ values and $K_{d\_receptor\_T}$ values confirms that $\Delta H_{a\_receptor\_T}$ does not change with temperature with regression coefficients not being significantly different to zero ($P > 0.19$) for binding of α2–3 and α2–6 sialyllactose to AIV HA monomer.

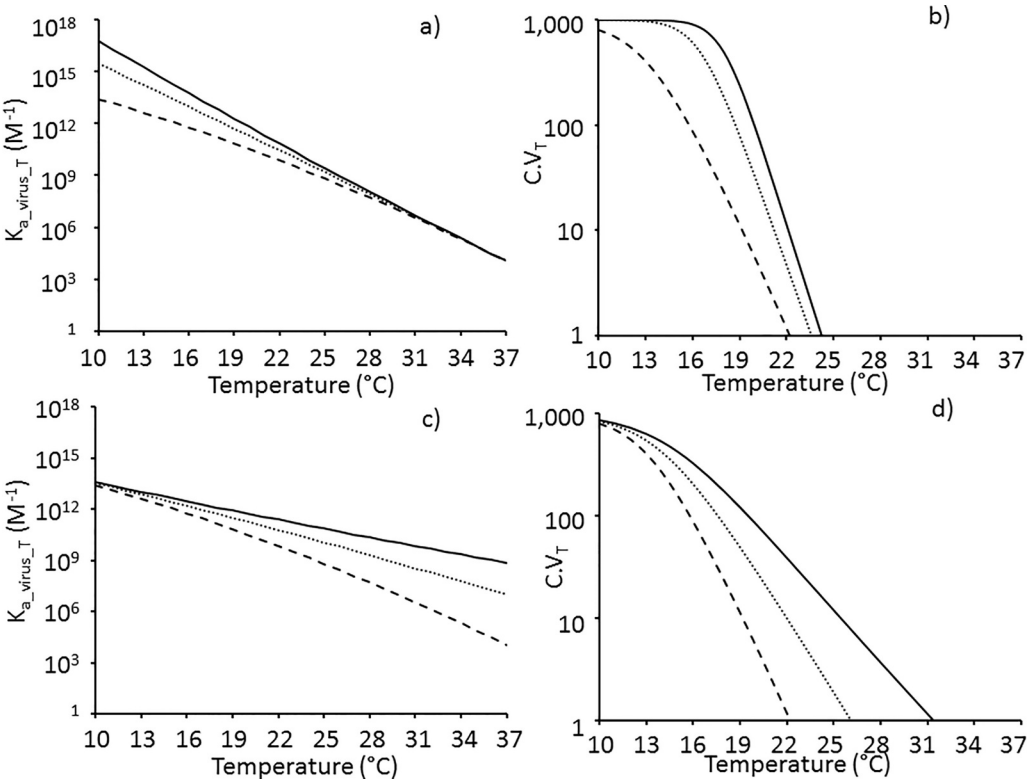

Fig. 4. Temperature variation of a) and c) $K_{a\_virus\_T}$ and b) and d) number, C.V_T, of CD4$^+$ *T* cells per mm^3 blood with bound HIV virions in HIV model for ΔC_p = 0 (solid line), −1.97 (dotted line) and −5.02 (dashed line) kJ/mol/K (Table 3) and thermodynamic parameters for n = 3 HIV Env:CD4 interactions in Table 4 at reference temperature a) and b) T_0 = 37 °C; c) and d) T_0 = 4 °C. ΔS_{a_immob} = −400 J/mol/K.

Myszka *et al.* (2000) at 25 °C (Table 4).

2.5.3. Thermodynamic parameters for HIV Env:CD4 binding at T_0 of 4 °C

Predicted values for $\Delta H_{a\_receptor\_T}$ and $\Delta S_{a\_receptor\_T}$ for HIV Env:CD4 binding at 4 °C are set out in Table 4 and are used as $\Delta H_{a\_receptor\_T0}$ and $\Delta S_{a\_receptor\_T0}$ respectively for the HIV model in Fig. 4c and d with the reference temperature, T_0, set to 4 °C to assess the effect of varying ΔC_p on the temperature sensitivity of $K_{a\_virus\_T}$ and C.V_T up to and above human body temperature.

2.5.4. Model for HIV binding to CD4$^+$ T cells in blood

The 2.5 to 97.5 percentile range for the number of CD4$^+$ *T* cells in humans is 448 to 1611 cells per mm^3 (10^{-6} dm^3) of blood with a mean of 919 cells per mm^3 (Thakar *et al.*, 2011). The model here takes 1 mm^3 of blood with $C_{total} = 10^3$ CD4$^+$ *T* cells and introduces $V_{total} = 10^5$ HIV virions. Dividing 10^5 HIV virions in 10^{-6} dm^3 by the Avogadro number gives $[V_{total}] = 1.7 \times 10^{-13}$ M. The advantage of using a high V_{total} that greatly exceeds C_{total} is that as previously demonstrated by Gale (2018) not only may the fraction, F_{cT}, of CD4$^+$ *T* cells with bound HIV be calculated from Eq. (13) with $[V_{free}] \sim [V_{total}]$ but also any complications of handling stochastic effects at low virus doses are avoided. It is recognised that the HIV concentration at 10^5 HIV virions per mm^3 used in this model is 10-fold to 100-fold higher than that expected in a recipient person's blood present in the capillaries lining the skin at the wound site where semen or blood from an infected source were introduced since maximum human plasma and human semen HIV loadings are in the region of 13,000 copies per mm^3 and 1800 copies per mm^3 respectively (Gupta *et al.*, 1997). This is not important, however, because the purpose of the models here in Figs. 4–6 is not to produce a realistic dose-response but to explore the effect of changing ΔC_p, ΔS_{a_immob}, n and temperature on the trend in the predicted number, C.V_T, of host CD4$^+$ *T* cells with bound virus. Indeed, the overall conclusions of the model in terms of the effect of temperature on the number of CD4$^+$ *T* cells with bound virus will still be representative and the interpretation applicable to all doses of viruses as there is no cooperation between viruses in this model (Gale 2018). Furthermore, the levels of SIV in Rhesus monkey blood plasma were in the region of 2.1×10^8 virions per ml (Huitron-Resendiz *et al.*, 2007) which is 2.1×10^5 virions per mm^3 and representative of the 10^5 used for $[V_{total}]$ in the model here. C.V_T is calculated by multiplying F_{cT} by C_{total} (Eq. (14)).

2.6. Case study 4: A large virus diameter such as for the HIV virion diminishes host cell binding at the higher temperatures of the human body through the large negative ΔS_{a_immob}

2.6.1. Estimation of ΔS_{a_immob} for a virus

There are currently no data available on the magnitude of ΔS_{a_immob} which was first defined through development of a thermodynamic model (Gale 2019). Xiong *et al.* (2013) reported a K_{d_virus} of 10^{-15} M for AIV where K_{d_virus} is the dissociation constant for virus from the host cell and is the inverse of $K_{a\_virus\_T}$. According to Yang *et al.* (2005) HIV virions bearing influenza A virus HA required 8 or 9 HA trimers for virus entry. This is equivalent to n = 24 to 27 HA monomers each of $K_{d\_receptor} = 10^{-3}$ M (Xiong *et al.*, 2013). It is not clear whether the 8 or 9 AIV HA trimers are required for cell binding or membrane fusion in Yang *et al.* (2005). However, if n = 24 HA monomers are required for AIV binding to the host cell to give a $K_{a\_virus\_T}$ of 10^{15} M^{-1} then ΔS_{a_immob} equals −1091 J/mol/K from Eq. (17) (derived in Gale 2019). This is in the same order of magnitude as assumed for ΔS_{a_immob} on the basis of virus molecular weight (Gale 2019). It must be emphasized that the estimate of 8 or 9 HA trimers in Yang *et al.* (2005) is based on a number of assumptions that may not hold, for example whereas each infection of a cell is a quantal, all-or-nothing event, the infectivity of a virion could span a wide spectrum of propensities and each mathematical model could have different virological interpretations (see Klasse 2012). However, in the absence of any data for ΔS_{a_immob} the value of n from Yang *et al.* (2005) at least provides a theoretical approach to estimate it from Eq. (17) for this “proof of concept” model.

2.6.2. Effect of virus size on the magnitude of ΔS_{a_immob}

It was shown previously (Gale 2019) that ΔS_{a_immob} is the sum of the

changes in translational entropy (ΔS_{trans}) and rotational entropy (ΔS_{rot}) of the whole virus on binding. According to Mammen *et al.* (1998) $\Delta S_{trans} \propto \ln(\text{Mass})$ and $\Delta S_{rot} \propto \ln(I_x \times I_y \times I_z)$ where I_x, I_y and I_z are the moments of inertia about the three principle axes of rotation. Since mass, M, is proportional to the volume and $I = Mr^2$ where r is the radius of the virus, it may be shown that the decrease in entropy on immobilisation (ΔS_{a_immob}) of a spherical virus can be expressed as Eq. (18).

Examples of diameters for arboviruses are ~50 nm for WNV (Mukhopadhyay *et al.*, 2003) and DENV, 66 nm for Eastern equine encephalitis virus (Hasan *et al.*, 2018) with BTV being slightly larger at 85 nm (Nason *et al.*, 2004). In contrast, HIV is much larger with a mean diameter of 134 nm in the case of mature HIV virions containing a single core (Briggs *et al.*, 2003). The problem with Eq. (18) is that proportionality constants in units of J/mol/K are needed probably based on R as in the Sackur-Tetrode equation and the natural logarithm terms should be dimensionless such that the units of radius cancel out. However for the purpose of representing the effect of increasing the radius of the virus on ΔS_{a_immob} Eq. (18) is used with the virus radius in units of nm. Thus from Eq. (18), the magnitude of ΔS_{a_immob} for a virus of diameter 134 nm is 18.6% more negative than that for a virus of diameter 66 nm. To illustrate the effect of increasing virus size on the number of $CD4^+$ *T* cells in 1 mm^3 of blood with bound virus, $C.V_T$ is calculated for the HIV model using values of ΔS_{a_immob} which decrease in steps of 18.6% from −240 J/mol/K (i.e. to −285 J/mol/K, −337 J/mol/K and −400 J/mol/K).

2.7. Case study 5: HIV attachment factors may partially overcome the unfavourable ΔS_{a_immob} and enhance specific virus binding through Env/CD4 interactions at human body temperature

2.7.1. Modelling the effect of non-specific binding of HIV to host $CD4^+$ T cells prior to specific Env:CD4 interaction

The term ΔS_{a_immob} represents the decrease in entropy of the virus on going from a freely rotating entity to being immobilised in a specific orientation on the host cell surface through $n = 3$ specific Env:CD4 interactions. Thermodynamically this could be accomplished in two consecutive steps whereby the virus first binds non-specifically to attachment proteins on the host cell surface with an entropy change of $\Delta S_{a\_non\_specific}$, and then rolls into place driven by $n = 3$ specific Env:CD4 interactions resulting in a further entropy loss ($\Delta S_{a\_specific}$) as the virus particle takes up a specific orientation ready for viral entry. In effect ΔS_{a_immob} is the sum of two components, namely $\Delta S_{a\_non\_specific}$ and $\Delta S_{a\_specific}$ according to Eq. (19). It should be noted that non-specific binding to HIV attachment factors would not increase ΔS_{a_immob} to zero because there are multiple ways a virus could bind non-specifically compared to the one way in which it binds to the CD4 receptors through a specific interaction between Env and CD4, that is the $\Delta S_{a\_specific}$ term is always negative i.e. <0 J/mol/K and $\Delta S_{a\_non\_specific}$ is always less negative than ΔS_{a_immob}.

Prior attachment through non-specific binding would realise the $\Delta S_{a\_non\_specific}$ loss before specific Env:CD4 binding so that specific binding involves the $\Delta S_{a\_specific}$ term alone. The value of ΔS_{a_immob} is estimated to be −1091 J/mol/K (see above) and for the purpose of demonstration here ΔS_{a_immob} is replaced by $\Delta S_{a\_specific}$ in Eq. (11) which is set to values of −400, −337, −285 and −240 J/mol/K in effect representing the effect of prior non-specific binding eliminating $\Delta S_{a\_non\_specific}$ values of −691, −754, −806 and −851 J/mol/K respectively according to Eq. (19).

2.8. Case study 6: Increasing the number, n, of GP/Cr contacts with temperature to reproduce the data of Frey et al. (1995) for binding of HIV Env-expressing cells to cells expressing CD4

Two outputs of the model are demonstrated. The first output builds on the model in Case study 5 with a $\Delta S_{a\_specific}$ of −206 J/mol/K to accommodate prior non-specific binding to attachment factors having eliminated the $\Delta S_{a\_non\_specific}$ of ~−900 J/mol/K. The model assumes $n = 3$ Env:CD4 interactions where n in Eq. (11) is increased from $n = 1$ to $n = 3$ with temperature between 25 °C and 27 °C (Fig. 6a) to represent the increase in contacts reported by Frey *et al.* (1995).

The second output attempts to include non-specific binding and also CCR5 co-receptor binding and a ΔS_{a_immob} of −1110 J/mol/K is used to represent the free virus binding (i.e. prior to non-specific binding). Kuhmann *et al.* (2000) demonstrated that approximately four to six CCR5 molecules assemble around the HIV virion to form a complex needed for infection. The model here assumes $n = 2$ non-specific Env interactions with attachment factors followed by $n = 4$ Env:CCR5 interactions according to Kuhmann *et al.* (2000) and finally $n = 3$ Env:CD4 interactions based on Brandenberg *et al.* (2015) to form a complex for binding with $n = 9$ contacts in total which increase from 1 to 9 with temperature as shown in Fig. 6b. Doranz *et al.* (1999) estimated the $K_{d\_receptor\_T}$ of interaction between CCR5 and HIV gp120 to be 4×10^{-9} M. This is remarkably similar to the $K_{d\_receptor\_T}$ for the interaction between CD4 and HIV Env of 4.75×10^{-9} M at 37 °C (Table 4) and the same values for $\Delta H_{a\_receptor\_T0}$ and $\Delta S_{a\_receptor\_T0}$ not only for the four HIV Env:CCR5 interactions but also for the two non-specific interactions are therefore used as for the three HIV Env:CD4 interactions in Table 4 with the reference temperature, T_0 at 37 °C.

3. Results

3.1. Published data on ΔC_p for GP/Cr binding and other protein-protein interactions

Published values of ΔC_p for protein/protein binding and for AIV HA binding to SA glycans vary in magnitude (Table 3). For the binding of HIV gp120 to CD4 which is a protein-protein interaction, the magnitude of $\Delta H_{a\_receptor\_T}$ becomes more negative as the temperature increases i.e. ΔC_p is negative (Fig. 1). Similarly, negative values of ΔC_p were reported for other protein-protein systems, namely the binding of E3 and E1 proteins, respectively, in the assembly of the enzyme pyruvate dehydrogenase (Jung *et al.*, 2002), although with ΔC_p values less negative than that for HIV gp120:CD4 (Table 3). In contrast for AIV HA binding to the SA glycan the magnitude of ΔC_p is not significantly different from zero with $\Delta H_{a\_receptor\_T}$ constant over the temperature range 15 °C to 25 °C at least for binding of both α2–3 and α2–6 sialyllactose (Fig. 1).

3.2. Case study 1: The predicted effect of the magnitude of ΔC_p on the temperature dependence of DENV transmission by Aedes albopictus

Values of $K_{a\_virus\_T}$ predicted over the temperature range of 10 °C to 37 °C using different values of ΔC_p intercept at the reference temperature (T_0) of 37 °C (Fig. 2a) with $K_{a\_virus\_T} = 10^{12}$ M^{-1} as expected for $n = 4$ GP/Cr interactions each of $K_{d\_receptor\_T0}$ of 10^{-3} M (Eq. (17)). With $\Delta C_p = 0$ kJ/mol/K as for AIV HA/SA, $K_{a\_virus\_T}$ increases with decreasing temperature according to the Van't Hoff Isochore. In contrast with $\Delta C_p = -5.02$ kJ/mol/K as for HIV gp120:CD4, $K_{a\_virus\_T}$ peaks at 26 °C and decreases rapidly at lower temperatures.

For the simulated DENV/*Ae. albopictus* model used here, small negative values of ΔC_p (−2.0 kJ/mol/K to 0 kJ/mol/K) have little effect on the probability of transmission at low temperatures (Fig. 2c,d). This is because in the model here with ΔC_p in the range of-2.0 kJ/mol/K to 0 kJ/mol/K, $K_{a\_virus\_T}$ is high at $>10^{14}$ M^{-1} at low temperatures (Fig. 2a) and thus $C.V_T$ is little affected until higher temperatures (Fig. 2b) at which $K_{a\_virus\_T}$ falls below 10^{14} M^{-1} (Fig. 2a). Large negative values of ΔC_p (−5.0 kJ/mol/K) cause $C.V_T$ to peak rapidly falling at lower temperatures (Fig. 2b). This has a large effect on the predicted probability of transmission at lower temperatures with $p_{transmissionT}$ 44-fold lower at 10 °C (Fig. 2d). It is interesting to note that ΔC_p has little effect on $p_{transmissionT}$ over the range of temperature (23 °C to 32 °C) at which laboratory vector competence experiments (Liu *et al.*,

2017b) are typically conducted (Fig. 2c).

3.3. Case study 2: The magnitude of ΔC_p could explain the temperature peak observed in the specific binding of WEEV to susceptible Culex tarsalis BBFs

With a $\Delta C_p = -3.0$ kJ/mol/K the magnitude of $K_{a\_virus\_T}$ between 0 and 40 °C is relatively constant compared to those with $\Delta C_p = 0$ kJ/mol/K and -5.02 kJ/mol/K (Fig. 3a) varying by only 40-fold and peaking at 1.62×13^{13} M^{-1} at 18 °C. However, this variation in $K_{a\_virus\_T}$ between 10^{12} and 10^{13} M^{-1} is optimal for affecting the number of midgut cells with bound virus (Fig. 3b). This is because $K_{a\_virus\_T}$ is high enough such that a significant proportion of midgut cells have bound virus over the 0 °C to 40 °C temperature range but not high enough to exceed the 10^{14} M^{-1} above which all the midgut cells are saturated with virus. The variation in $C.V_T$ with temperature with $\Delta C_p = -3.0$ kJ/mol/K shows some similarity to the percentage variation in the amount of WEEV bound to BBFs from susceptible *Culex tarsalis* mosquitoes as measured experimentally by Houk *et al.* (1990) as represented by the symbols in Fig. 3b. According to Houk *et al.* (1990) the $K_{a\_virus\_T}$ at 20 °C for WEEV binding to BBFs from susceptible *Culex tarsalis* mosquitoes is 2.2×10^{11} M^{-1}. This is within two orders of magnitude of the value of 1.57×10^{13} M^{-1} predicted by the model here with $\Delta C_p = -3.0$ kJ/mol/K (Fig. 3a).

3.4. Case study 3: A large negative ΔC_p for a protein:protein GP/Cr system as represented by HIV gp120:CD4 diminishes host cell binding at higher temperature

3.4.1. Reference temperature, T_0, equals 37 °C

$K_{a\_virus\_T}$ values for HIV binding and $C.V_T$ values for the number of $CD4^+$ *T* cells in 1 mm^3 of blood with bound HIV as a function of temperature are shown in Fig. 4a and b respectively for different ΔC_p values with $T_0 = 37$ °C. The $K_{a\_virus\_T}$ and $C.V_T$ values in Fig. 4a and b respectively assume $n = 3$ Env:CD4 contacts with thermodynamic parameters in Table 4 and $\Delta S_{a\_immob} = -400$ J/mol/K. The large negative value of ΔC_p of -5.02 kJ/mol/K reported for gp120:CD4 (Table 3) diminishes binding at higher temperatures compared to ΔC_p of 0 kJ/mol/K. Thus from Fig. 4b, only half of the 1000 cells have bound virus at 12 °C with $\Delta C_p = -5.02$ kJ/mol/K while with $\Delta C_p = 0$ kJ/mol/K half the cells still have bound virus at a temperature of 6 °C higher (18 °C). With $\Delta C_p = -5.02$ kJ/mol/K, $C.V_T$ is <1 cell (i.e. no virus bound) at 22 °C while with $\Delta C_p = 0$ kJ/mol/K the slightly higher temperature of 24 °C is required to decrease $C.V_T$ to <1 cell (Fig. 4b).

3.4.2. Effect of changing the reference temperature, T_0, from 37 °C to 4 °C

The three lines representing $K_{a\_virus\_T}$ for different values of ΔC_p in Fig. 4a intercept at 37 °C (T_0) and would do for $C.V_T$ in Fig. 4b if extrapolated to 37 °C. To demonstrate how the magnitude of ΔC_p affects $K_{a\_virus\_T}$ at temperatures of 37 °C representing mammalian body temperature, the reference temperature is set to 4 °C such that the three plots for $K_{a\_virus\_T}$ intercept at 4 °C in Fig. 4c with much lower $K_{a\_virus\_T}$ values predicted at 37 °C with a large negative ΔC_p than for a system with $\Delta C_p = 0$ kJ/mol/K. The effect of ΔC_p on the number of cells with bound virus at higher temperatures is considerable with $C.V_T$ reduced to 1 cell at 22 °C with $\Delta C_p = -5.02$ kJ/mol/K compared to 31 °C with $\Delta C_p = 0$ kJ/mol/K (Fig. 4d).

It should be noted that the dashed lines in Fig. 4c and d are the same as those in Fig. 4a and b respectively being based on experimental data for HIV gp120:CD4 (Fig. 1). The purpose of the dotted and solid lines is merely to illustrate the effect of less negative ΔC_p increasing the binding at higher temperatures for the purpose of understanding.

3.5. Case study 4: A large virus diameter as for the HIV virion diminishes host cell binding at the higher temperature of the human body through the large negative ΔS_{a_immob}

From Eq. (18), ΔS_{a_immob} becomes more negative as the diameter of the virus increases. The value of $K_{a\_virus\_T}$ decreases with increasing temperature in Fig. 5a while more negative values of ΔS_{a_immob} merely shift each parallel curve to lower $K_{a\_virus\_T}$ values as expected from Eq. (17) such that $K_{a\_virus\_T}$ falls below 10^{14} M^{-1} at progressively lower temperatures. Values of $C.V_T$ with ΔS_{a_immob} decreasing from -240 J/mol/K to -400 J/mol/K in steps of 18.6% are plotted in Fig. 5b and show that the number of cells with bound virus falls to <1 at progressively lower temperature as ΔS_{a_immob} becomes more negative through increasing the virus diameter. The temperature at which $C.V_T$ falls to <1 is predicted to increase from 22 °C to 43 °C as ΔS_{a_immob} increases in magnitude from -400 J/mol/K to -240 J/mol/K. The conclusion from Fig. 5a and b is that smaller viruses with less negative ΔS_{a_immob} bind more strongly at higher temperatures than larger viruses. Only with ΔS_{a_immob} as high as -240 J/mol/K representing smaller viruses do more than 30% of the 1000 cells have bound virus at the human body temperature of 37 °C according to the model in Fig. 5b. This is shown in Fig. 5c where nearly all the cells have bound virus at 10 °C irrespective of ΔS_{a_immob} while at higher temperatures fewer cells have bound virus as ΔS_{a_immob} becomes more negative.

3.6. Case study 5: HIV attachment factors may partially overcome the unfavourable ΔS_{a_immob} and enhance specific virus binding through Env/CD4 interactions at human body temperature

Fig. 5 can also be interpreted in terms of the effect of prior non-specific binding of HIV to attachment factors eliminating $\Delta S_{a\_non\_specific}$ values of -691, -754, -806 and -851 J/mol/K according to Eq. (19) thus increasing $\Delta S_{a\_specific}$ for specific Env:CD4 binding (as ΔS_{a_immob} in Eq. (11)) from -400 J/mol/K to -240 J/mol/K. Fig. 5b shows that the number of $CD4^+$ *T* cells in a 1 mm^3 vol of blood with bound HIV falls from 1000 to <1 over a temperature range of ~10 °C. The temperature at which fewer than half the T cells in the 1 mm^3 vol of blood have bound HIV virus increases with increasing $\Delta S_{a\_specific}$ from 12.5 °C for $\Delta S_{a\_specific} = -400$ J/mol/K to 36.5 °C for $\Delta S_{a\_specific} = -240$ J/mol/K (Fig. 5b). Indeed once the $\Delta S_{a\_specific}$ is > -200 J/mol/K, 98% of the 1000 T cells have bound HIV at 37 °C (not shown). With $\Delta S_{a\_specific}$ < -285 J/mol/K virus is not specifically bound to any of the 1000 T cells at temperatures above 37 °C. It is concluded that the effect of making ΔS_{a_immob} less unfavourable through prior non-specific binding taking some of the entropy loss enhances subsequent specific binding of HIV through Env:CD4 interactions at higher temperatures. Fig. 5c shows that at 37 °C increasing $\Delta S_{a\_specific}$ from -400 to -240 J/mol/K increases the number of $CD4^+$ *T* cells with HIV bound through specific Env/CD4 interactions in a 1 mm^3 vol of blood from 2×10^{-6} to 307. It should be noted that 2×10^{-6} cells in 1 mm^3 is equivalent to 1 cell in 500 cm^3 of blood.

3.7. Case study 6: Increasing the number, n, of GP/Cr contacts with temperature to reproduce the data of Frey et al. (1995) for binding of HIV Env-expressing cells to cells expressing CD4

Cells expressing HIV Env on their surface can bind and fuse with cells expressing CD4 Cr (Frey *et al.*, 1995). Frey *et al.* (1995) reported a three to four fold increase in cell binding at temperatures above 25 °C with a substantial decrease in binding at temperatures above 37 °C (Fig. 6), the latter being predicted by the thermodynamic model in Fig. 5b. Frey *et al.* (1995) attribute the increase at 25 °C to the additional adhesion molecules which are brought into contact to increase the avidity of binding at higher temperatures. The thermodynamic model for HIV binding with ΔS_{a_immob} of -206 J/mol/K reproduces the increase in predicted $C.V_T$ in Fig. 6a by increasing n from 1 to 3 over the

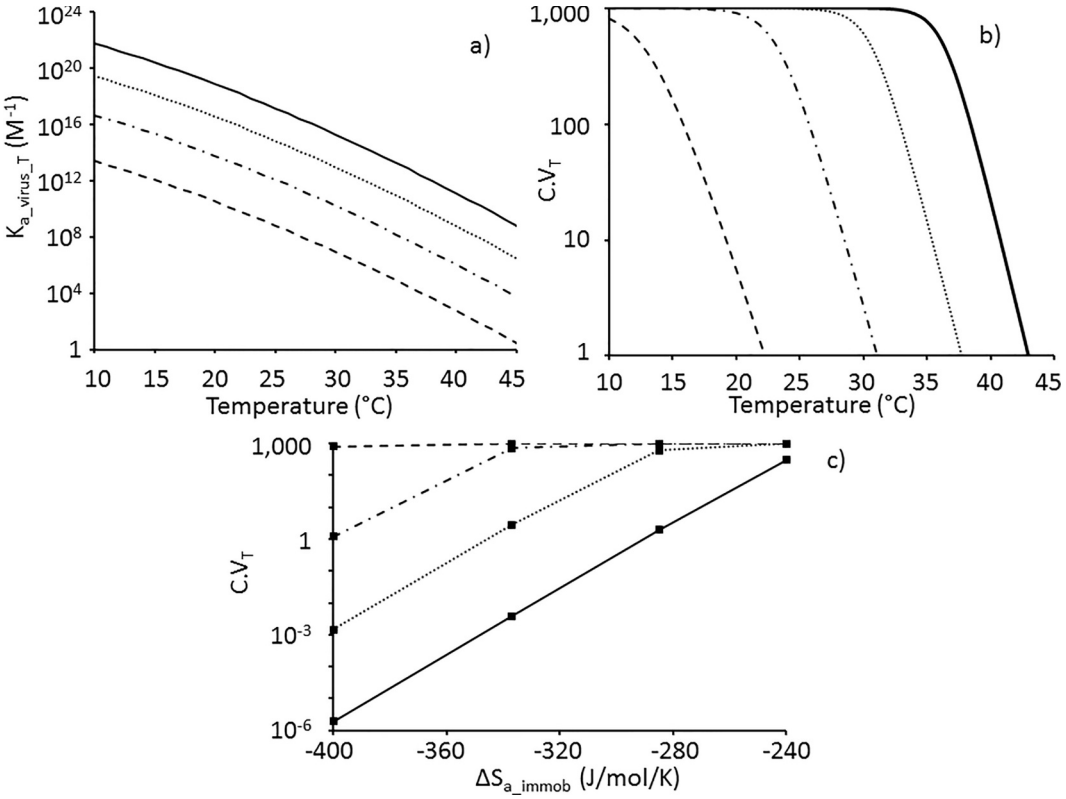

Fig. 5. Predicted effect of ΔS_{a_immob} on the temperature sensitivity of a) $K_{a\_virus\_T}$ and b) the number of host $CD4^+$ *T* cells, $C.V_T$, with bound HIV virions in a system comprising $C_{total} = 10^3$ $CD4^+$ host *T* cells in a 1 mm^3 vol of blood with a challenge dose of 10^5 HIV virions. The values of $\Delta H_{a\_receptor\_T0}$ and $\Delta S_{a\_receptor\_T0}$ at $T_0 = 37$ °C for specific HIV Env:CD4 binding are given in Table 4 with $n = 3$ Env:CD4 specific interactions and $\Delta C_p = -5.02$ kJ/mol/K (Table 3) for $\Delta S_{a\_immob} = -400$ J/mol/K (dashed line), -337 J/mol/K (dash-dotted line), -285 J/mol/K (dotted line) and -240 J/mol/K (solid line). c) Effect of ΔS_{a_immob} on $C.V_T$ predicted at temperatures of 10 °C (dashed line), 22 °C (dash-dotted line), 30 °C (dotted line) and 37 °C (solid line) with symbols representing outputs from model. For case study 4, more negative values of ΔS_{a_immob} represent virions of increasing diameter. For case study 5, non-specific HIV attachment factor interactions prior to the specific HIV Env:CD4 interactions make ΔS_{a_immob} less negative through realising entropy loss of $\Delta S_{a\_non\_specific}$ in Eq. (19) (see text).

temperature range 25 °C and 27 °C to reflect the effect of temperature facilitating multiple HIV adhesion/binding sites due to increased membrane fluidity (Frey *et al.*, 1995; Harada *et al.*, 2004). Increasing n from 1 to 9 over the temperature range 19 °C and 27 °C gives a sharp increase in $C.V_T$ at 26 °C (Fig. 6b) with ΔS_{a_immob} of -1110 J/mol/K. The subsequent sharp fall in $C.V_T$ at temperatures above 37 °C is due to the large negative magnitude of ΔS_{a_immob} (-206 J/mol/K in Fig. 6a and -1110 J/mol/K in Fig. 6b) relative to n such that the diminished GP/Cr affinity at higher temperatures is not sufficient to maintain binding even with $n = 9$ GP/Cr interactions in Fig. 6b. The decrease in GP/Cr binding affinity with temperature for HIV Env:CD4 is apparent from the $K_{a\_virus\_T}$ values in Fig. 5a and the increase in the values of $K_{d\_receptor\_T}$ for the temperatures 4 °C, 25 °C and 37 °C in Table 4.

4. Discussion

Previously a thermodynamic model for the effect of temperature on arthropod vector competence was developed (Gale 2019) based on the parameters $\Delta H_{a\_receptor\_T}$, $\Delta S_{a\_receptor\_T}$, ΔS_{a_immob} and n, together with the kinetic parameters, $p_{complete283}$ and E_A (Table 2). This paper furthers that model by allowing the change in heat capacity, ΔC_p, on GP/Cr binding to be included. This is important because it defines the effect of temperature on $\Delta H_{a\_receptor\_T}$ (Eq. (4)) and $\Delta S_{a\_receptor\_T}$ (Eq. (6)) and hence $K_{a\_virus\_T}$. Of potentially greater importance, however, is the parameter ΔS_{a_immob} first formally identified in the thermodynamic analysis of virus binding (Gale 2019). Thus it is proposed here that the value of ΔS_{a_immob} is not only important in explaining the observation that dsDNA viruses infecting warmer hosts are generally smaller in volume than those infecting colder hosts (Nifong and Gillooly 2016) but also may contribute to explaining the need for attachment factors to allow binding of a large virus such as HIV at the relatively high human body temperature of 37 °C. This has implications for the design of novel antiviral therapies. The mechanistic model developed here for HIV goes as far as cell binding and viral membrane fusion (Harrison 2015) could be added as the next stage to complete the cell entry process.

4.1. Justification of assumptions for ΔS_{a_immob}

Calculations using Eq. (17) on the basis of limited available data suggest $\Delta S_{a\_immob} \sim -1100$ J/mol/K for HIV although it is acknowledged above that there is considerable uncertainty in the absence of definitive experimental data. It is possible that statistical thermodynamics approaches analogous to the Sackur-Tetrode equation for the entropy of a gas may be developed to estimate ΔS_{a_immob} theoretically. The large size of the HIV virion (134 nm mean diameter) compared to a typical arbovirus (50 to 70 nm diameter) is consistent with a more negative value of ΔS_{a_immob} providing justification for the more negative ΔS_{a_immob} values used here for the HIV models in Figs. 4–6 compared to that used for the arbovirus models in Figs. 2 and 3.

4.2. Interpretation of figures

Figs. 2–5 show the variation of $K_{a\_virus\_T}$ and $C.V_T$ with temperature as predicted by models assuming $C_{total} = 10^3$ host cells in a 10^{-6} dm^3 volume (i.e. mosquito midgut or human blood sample) challenged with $V_{total} = 10^5$ virions. Previously it was shown that if $K_{a\_virus\_T} > \sim 10^{14}$ M^{-1} then nearly all the host cells have bound virus at such a high virus dose (Gale 2018; 2019). Thus the $K_{a\_virus\_T}$ plots and corresponding $C.V_T$

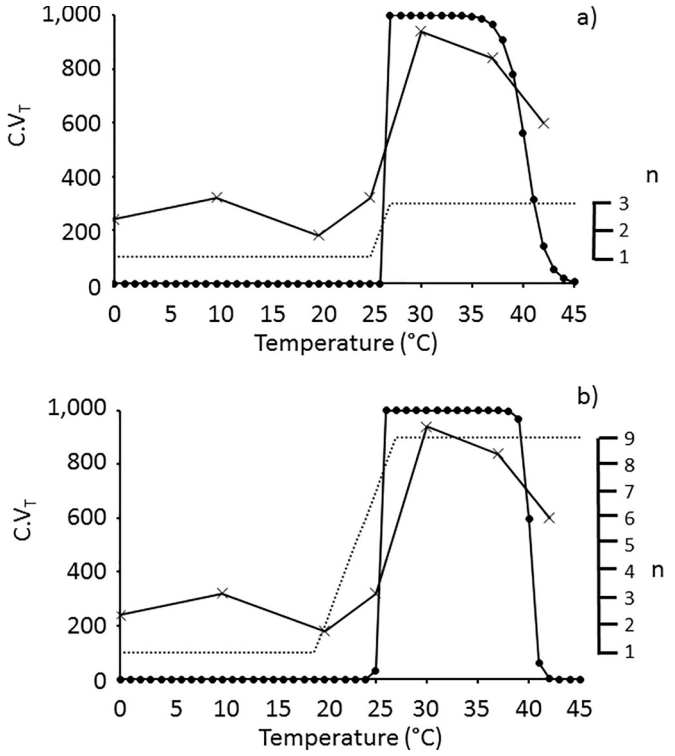

Fig. 6. Experimental binding of HIV Env-expressing cells to cells expressing CD4 as reported by Frey *et al.* (1995) increases three to four fold at 25 °C (cross). The number, C.V_T, of $CD4^+$ *T* cells with bound HIV virions per mm^3 blood predicted by the thermodynamic model (circle) using Eq. (11) with the number, n, of GP/Cr contacts increasing according to the dotted line with temperature in a) from 1 to 3 between 25 and 27 °C; and in b) from 1 to 9 between 19 °C and 27 °C. The values of $\Delta H_{a\_receptor\_T0}$ and $\Delta S_{a\_receptor\_T0}$ at T_0 = 37 °C for non-specific attachment factor binding and for HIV Env:CCR5 co-receptor binding are as those for specific HIV Env:CD4 binding in Table 4 with ΔC_p = −5.02 kJ/mol/K (Table 3). ΔS_{a_immob} = *a*) −206 J/mol/K to represent prior elimination of $\Delta S_{a\_non\_specific}$ through binding of virus through non-specific attachment; and b) −1,110 J/mol/K to represent free virus binding.

plots are best interpreted in terms of the temperature ranges over which $K_{a\_virus\_T} < \sim 10^{14}\ M^{-1}$.

4.3. The importance of negligible ΔC_p for low temperature arbovirus transmission

For the arbovirus models in Figs. 2 and 3, the main conclusion regarding the change in heat capacity on GP/Cr binding is that as ΔC_p becomes more negative so a peak temperature for $K_{a\_virus\_T}$ becomes apparent such that binding affinity falls at lower and higher temperatures, directly affecting C.V_T when $K_{a\_virus\_T}$ falls below $10^{14}\ M^{-1}$. Values of ΔC_p from 0 to ~−2.0 kJ/mol/K have relatively little impact on the temperature sensitivity of the number, C.V_T, of mosquito midgut cells with bound virus (Fig. 2b), while intermediate values of ΔC_p of ~−3.0 kJ/mol/K give a peak binding at a temperature of ~20 °C as observed experimentally for WEEV binding to BBFs from susceptible mosquito midguts in Fig. 3b. More negative values of ΔC_p at −5.0 kJ/mol/K greatly diminish arbovirus binding affinity at temperatures below ~20 °C (Fig. 2b) which in turn diminishes the transmission efficiency of the arbovirus at temperatures below 20 °C compared to GP/Cr systems with ΔC_p in the range of −2.0 to 0 kJ/mol/K (Fig. 2d). In evolutionary terms, to optimise arbovirus infectivity with n = 4 GP/Cr interactions over a range of temperatures, GP/Cr interactions with small ΔC_p would be selected as for AIV HA/SA binding (Table 3). It is proposed here that to maintain some transmission efficiency at lower temperatures, arboviruses may use SA binding interactions as shown for BTV coat protein VP2 (Zhang *et al.*, 2010) for which ΔC_p may approximate 0 kJ/mol/K as in the case of AIV HA/SA (Table 3). This would facilitate arboviruses' expanding their range into temperate regions of the world with climate change.

4.3.1. The value of ΔC_p does not affect arbovirus binding to arthropod midguts at higher temperatures

With the reference temperature of T_0 = 37 °C, C.V_T falls rapidly at temperatures above 20 °C in the arbovirus model here with n = 4 GP/Cr interactions irrespective of the magnitude of ΔC_p (Fig. 2b) as the $K_{a\_virus\_T}$ values fall below $10^{14}\ M^{-1}$ and converge at $10^{12}\ M^{-1}$ at 37 °C (Fig. 2a). This fall is observed experimentally as the temperature is increased from 20 °C to 40 °C (Fig. 3b) for WEEV binding to BBFs from susceptible mosquito midguts as reported by Houk *et al.* (1990).

4.4. The large negative ΔC_p for HIV gp120:CD4 diminishes binding at human body temperature in the HIV model

The ΔC_p for HIV gp120:CD4 binding is well documented unlike that for arbovirus binding and the values of $\Delta H_{a\_receptor\_T}$ have been reported over the temperature range of 12 °C to 44 °C (Fig. 1). The results with varying ΔC_p in Fig. 4 are therefore hypothetical but illustrate how the large negative ΔC_p for the HIV Env:CD4 interaction diminishes binding at the higher temperatures of mammals and birds compared to a system such as HA/SA for which ΔC_p = 0 kJ/mol/K. Thus, a less negative ΔC_p increases the number of cells with bound virus at higher temperatures, albeit more markedly for the reference temperature T_0 = 4 °C (Fig. 4d) than for T_0 = 37 °C (Fig. 4b). In the absence of data for ΔC_p for HIV Env:CD4 binding, the value for the gp120 monomer:CD4 interaction is used for the HIV models in Figs. 4–6. Evidence for a large negative ΔC_p for HIV Env:CD4 binding is that cryo-EM demonstrates considerable conformational shifts (Liu *et al.*, 2017a).

4.5. ΔS_{a_immob} as a repulsive force in virus binding

A negative value of ΔS_{a_immob} presents a repulsive force between the virus and the host cell in effect preventing virus binding and with n = 0 GP/Cr contacts, $K_{a\_virus\_T}$ is $< 1\ M^{-1}$ according to Eq. (17) (Gale 2019). Increasing the value of n is one way for the virus to overcome a large negative value of ΔS_{a_immob} (Gale 2019). Thus 15 to 18 GP/Cr contacts of $K_{d\_receptor\_T0} = 10^{-3}$ M (37 °C) were sufficient to overcome a ΔS_{a_immob} of −750 J/mol/K such that $K_{a\_virus\_T} > 10^{14}\ M^{-1}$ (Fig. 3 of Gale (2019)). This is apparent from Fig. 6a where n = 3 GP/Cr contacts can overcome a ΔS_{a_immob} of −206 J/mol/K while n = 9 GP/Cr contacts are required to overcome the more negative ΔS_{a_immob} of −1110 J/mol/K in Fig. 6b.

4.6. A less negative ΔS_{a_immob} maintains virus binding at higher temperatures

Even for ΔS_{a_immob} = 0 J/mol/K as in Figs. 2a and 3a, the magnitude of $K_{a\_virus\_T}$ decreases with increasing temperature (albeit after a peak in the case of $\Delta C_p < -2.0$ kJ/mol/K). This is due to the reduced affinity of the enthalpy-driven GP/Cr interactions at higher temperatures. Making ΔS_{a_immob} more negative shifts the $K_{a\_virus\_T}$ curve to lower values (Fig. 5a) thus exacerbating the effect of higher temperature on reducing binding. As $K_{a\_virus\_T}$ falls below $10^{14}\ M^{-1}$ at higher temperatures, so C.V_T falls (Fig. 5b). The magnitude of ΔS_{a_immob} merely positions the C.V_T curve relative to the temperature scale with less negative values of ΔS_{a_immob} shifting the curve to higher temperatures (Fig. 5b) such that high C.V_T values are maintained at progressively higher temperatures as ΔS_{a_immob} becomes less negative (Fig. 5c).

4.7. Balancing opposing constraints at mammalian host temperatures

The thermodynamic model here suggests that a large negative ΔC_p for HIV Env:CD4 diminishes binding at higher temperatures. However,

there may be molecular constraints such that a large negative ΔC_p value is a direct consequence of a molecular mechanism involving a large conformational change that serves a purpose for cell entry/fusion (Harrison 2015) such that a negligible ΔC_p value may not be achievable. Furthermore, a large negative ΔS_{a_immob} imposes additional constraints on virus binding at higher temperatures exacerbating the reduced strength of the enthalpy-driven GP/Cr interactions at higher temperatures. Therefore other mechanisms may be needed by the virus to achieve binding at 37 °C. These could include more GP/Cr contacts at higher temperature (Frey *et al.*, 1995; Harada *et al.*, 2004). An alternative strategy evolved by viruses could be to make ΔS_{a_immob} itself less negative such that virus binding is maintained at the higher body temperatures of mammals and birds. Two possible evolutionary strategies are suggested here which could make ΔS_{a_immob} less negative. The first is decreasing the size of the virus and the second is the use of non-specific attachment factors to randomly trap the virus on the cell surface prior to specific GP/Cr binding.

4.8. Small virus size makes ΔS_{a_immob} less negative thus maintaining binding at higher temperatures

Decreasing the size of a virus makes ΔS_{a_immob} less negative (Eq. (18)) such that smaller viruses bind more strongly at the higher temperatures of mammals and birds (Fig. 5). It is suggested that binding to cells at the higher temperatures of avian and mammalian hosts selects for viruses of smaller diameter through a less negative ΔS_{a_immob}. This could explain the decrease in volume of viruses with increasing host/environment temperature as reported by Nifong and Gillooly (2016) for dsDNA viruses. Thus the average diameters of dsDNA viruses decreased from 182 nm at a host/environment temperature of 10 °C down to 74 nm at 37 °C according to the best fit line of Nifong and Gillooly (2016) suggesting the HIV virion at 134 nm mean diameter is almost double the size for a virus infecting at avian/mammalian host temperature. It is interesting to note that thermophilic bacteria adapted to high temperature may be subject to selection favouring smaller cell size. This may aid attachment to biofilms which provide some protection against temperature stress.

4.9. The importance of prior non-specific binding in taking some of the entropy loss in ΔS_{a_immob}

It is proposed here that by taking the entropy loss $\Delta S_{a\_non\_specific}$ in ΔS_{a_immob} that non-specific binding to attachment factors facilitates subsequent specific HIV Env binding to CD4 receptors on the host $CD4^+$ *T* cell at human body temperature. Thus the shift in the $K_{a\_virus\_T}$ curve to higher values with a less negative ΔS_{a_immob} in Fig. 5a is consistent with HIV attachment factors augmenting infection (Wilen *et al.*, 2012). Indeed with $n = 3$ Env:CD4 contacts, significant binding of HIV to host cells is only achieved at 37 °C if ΔS_{a_immob} is increased to > -280 J/mol/K (Fig. 5c). ΔS_{a_immob} is estimated here to be -1091 J/mol/K for HIV. Thus the prior non-specific binding of HIV would need to realise a $\Delta S_{a\_non\_specific}$ of -810 J/mol/K for subsequent effective Env:CD4 binding at human body temperature according to the model such that $\Delta S_{a\_non\_specific}$ in Eq. (19) takes ~75% of the entropy loss in ΔS_{a_immob}. Wilen *et al.* (2012) also report that HIV attachment factors are not essential. Again this is consistent with the model here when it is noted that the $C.V_T$ value of <1 $CD4^+$ *T* cell with bound virus in Fig. 5b is not a threshold and merely represents 1 mm^3 of blood. Thus with $\Delta S_{a\_immob} = -348$ J/mol/K, $C.V_T = 1 \times 10^{-3}$ at 37 °C (Fig. 5c). This represents one $CD4^+$ *T* cell with bound HIV in 1000×1 mm^3 vol of blood, i.e. in 1 cm^3 of blood. Decreasing ΔS_{a_immob} further to -405 J/mol/K gives $C.V_T = 1 \times 10^{-6}$ at 37 °C representing one $CD4^+$ *T* cell with bound HIV in 1 litre of blood.

4.10. Making ΔS_{a_immob} more negative as a strategy for development of antiviral therapeutics

The model here suggests human body temperature may be a constraint on HIV binding (due to the large negative values of both ΔC_p and ΔS_{a_immob}) in effect exposing a potential weakness in the HIV infection strategy which could be exploited for antiviral therapy. Figure 9 of Antoine *et al.* (2012) shows a herpes simplex virus type 2 (HSV-2) bound to a tetrahedral nanoparticle of zinc oxide (ZnO) called a zinc oxide tetrapod (ZnOT). The mechanism behind the ability of ZnOTs to prevent, neutralize or reduce HSV-2 infection relies on their ability to bind the HSV-2 virions (Antoine *et al.*, 2012). The ZnOT being some 40 μm in size is much larger than the attached virion which could still attach to a host cell surface in terms of spatial considerations. However, the magnitude of ΔS_{a_immob} for an HSV-2 virion bound to a ZnOT nanoparticle would be very large and negative, indeed much more negative than for ΔS_{a_immob} for a free HSV-2 virion. Thus according to Fig. 5c, binding of HSV-2/ZnOT to host cells would be greatly diminished particularly at the human body temperature due to the very large negative ΔS_{a_immob}. Although ΔS_{a_immob} changes logarithmically (i.e. slowly) with virus size according to Eq. (18), the number, $C.V_T$, of cells with bound virus is very sensitive to changes in ΔS_{a_immob} at 37 °C (Fig. 5c). It is proposed that antiviral research should take into account and even focus on making the magnitude of ΔS_{a_immob} more negative in addition to looking at conventional approaches to block the GP/Cr interaction. The advantage of focusing on ΔS_{a_immob} is that only one ZnOT nanoparticle has to bind to a virus to markedly affect ΔS_{a_immob}, while a large proportion of the GP molecules on the virus have to be bound with inhibitors, including neutralising antibodies, to block virus binding (Klasse 2012) and hence eliminate $\Delta H_{a\_receptor\_T0}$ in Eq. (11). The temperature dependence of virus diffusion in mucus (Erickson *et al.*, 2015) could also be considered not only in mechanistic dose-response models for viral infection at mucosal epithelial membranes in the intestine (Gale 2018) but also in terms of therapeutics when combined with the thermodynamic approach developed here. Normal, acidic cervicovaginal mucus greatly hinders the movement of virions of HSV and HIV, whereas mucus that is neutralized by semen provides a much less effective barrier against the same virions (Erickson *et al.*, 2015). Thus binding of the HSV or HIV virion to a ZnOT particle may not only decrease its diffusion coefficient in mucus but also make the magnitude of ΔS_{a_immob} more negative hence reducing the binding affinity of those virions which do make it through the mucus to the epithelial cell surface at human body temperature.

4.11. Validation of the HIV model

It is assumed for the purpose of the "proof of concept" model here that the thermodynamic parameters for the HIV gp120 monomer:CD4 interaction in Myszka *et al.* (2000) can be used for HIV Env trimer binding to a single CD4 in the absence of data. Although the $K_{d\_receptor\_T}$ value for the Env trimer:CD4 interaction (1.4×10^{-9} M, Chuang *et al.*, 2017) is 15-fold higher than that for the gp120 monomer:CD4 interaction (0.9×10^{-10} M, Table 4) at 25 °C, this is close enough to support using the gp120 monomer:CD4 data, particularly as $K_{d\_receptor\_T}$ values for the gp120 monomer:CD4 interaction vary nine-fold between two HIV strains (see above).

The predicted values of $K_{a\_virus\_T}$ increase with decreasing temperature according the HIV model in Fig. 5a. This is unexpected on the basis of the $\Delta H_{a\_receptor\_T}$ values reported by Myszka *et al.* (2000) for gp120:CD4 which become less negative with decreasing temperature (Fig. 1). However, according to Eq. (6) the predicted $\Delta S_{a\_receptor\_T}$ term becomes more favourable (less negative) with decreasing temperature and it is therefore the entropy term that facilitates the tighter binding of gp120 to CD4 at lower temperatures. Unfortunately Myszka *et al.* (2000) only give the full range of values for $\Delta H_{a\_receptor\_T}$ (Fig. 1) with no data for $\Delta S_{a\_receptor\_T}$ over the range of temperature. However,

Myszka *et al.* (2000) do give some graphical data from which $\Delta S_{a\_receptor\_T}$ at 25 °C can be estimated and it is reassuring this $\Delta S_{a\_receptor\_T}$ is much less negative at −473 J/mol/K than that of −691 J/mol/K measured at 37 °C and furthermore is actually less negative than the value of −492.8 J/mol/K predicted for 25 °C by Eq. (6) (Table 4) and used in the model in Fig. 5. This is strong experimental evidence that warming to 37 °C and above does indeed give a significant reduction in the binding affinity of Env to CD4 as borne out by the 52-fold increase in the $K_{d\_receptor\_T}$ value for gp120:CD4 on warming from 25 °C to 37 °C as calculated from the actual data of Myszka *et al.* (2000) (Table 4). Furthermore it suggests that the actual increase in $K_{a\_virus\_T}$ on cooling from 37 °C down to 25 °C may be greater than that predicted by the model in Fig. 5a. The decrease in binding affinity with increasing temperature for HIV Env:CD4 is also supported by experimental data of Moore and Klasse (1992) which showed that soluble CD4 dissociated from HIV virions at temperatures above 35 °C. Similarly Doranz *et al.* (1999) demonstrated that gp120 bound to $CD4^+$ *T* cells began to dissociate at temperatures above 45 °C. The data of Frey *et al.* (1995) in Fig. 6 offer further validation of the model in that the binding of HIV Env-expressing cells to cells expressing CD4 decreases substantially at 37 °C as predicted by the model. The Env trimer is stable up to at least 60 °C (Chuang *et al.*, 2017) suggesting it is not denaturation of the Env trimer itself that is responsible for the decreased binding at higher temperatures. However, care has to be taken in using Eqs. (4) and (6) to predict $\Delta H_{a\_receptor\_T}$ and $\Delta S_{a\_receptor\_T}$ respectively down to very low temperatures. Thus although the predicted value of $K_{d\_receptor\_T}$ for gp120:CD4 at 4 °C is 3700-fold lower than that at 37 °C (Table 4), Frey *et al.* (1995) cite some studies which suggested weaker binding of soluble CD4 to HIV virions at 4 °C compared to 37 °C. Without actual binding data for HIV over the full temperature range, it cannot be ruled out that $K_{a\_virus\_T}$ does not exhibit a peak with temperature as for the WEEV binding in Fig. 3b. Indeed, binding of ^{125}I-labelled gp120 to T cells peaked at 16 °C with binding at 4 °C much lower than that at 37 °C (Frey *et al.*, 1995). The observed increase between 4 °C and 16 °C is unlikely to be due to increased fluidity of the membrane allowing recruitment of more CD4 molecules because unlike the virus, each gp120 only binds a single Cr molecule. Dimitrov *et al.* (1992) showed that the activation energy for binding of soluble CD4 to cells expressing HIV Env changed at 18 °C suggesting 18 °C is a transition temperature. This could explain the peak in binding of gp120 at 16 °C reported by Frey *et al.* (1995). Thus extrapolation of $\Delta H_{a\_receptor\_T}$ and $\Delta S_{a\_receptor\_T}$ through Eqs. (4) and (6), respectively to temperatures below 18 °C may not be justified in the case of HIV binding.

It should be remembered that HIV only infects humans at 37 °C and therefore the lower temperature predictions are more of academic interest, although temperature trends may give an insight into weaknesses in the HIV infection strategy as suggested here. It is only the 37 °C line in Fig. 5c which is important for HIV and it is reassuring to note that this is based on actual experimental data for gp120 monomer:CD4 binding measured at that temperature. The lower temperature lines in Fig. 5c are of more general interest, for example in explaining the observed relationship (Nifong and Gillooly 2016) between larger virus volume and lower host temperature.

4.12. Variation between virions in an exposure dose

Individual virions of the same virus may vary both in size (Briggs *et al.*, 2003) and in the case of some RNA viruses in the actual base sequence of the genome giving a spectrum of mutants. The infection process may represent a bottleneck such that only one or two viral variants in the exposure dose successfully establish infection (Bull *et al.*, 2011). Thus in the case of norovirus, only minor variants at frequencies as low as 0.01% were successfully transmitted to establish a new infection (Bull *et al.*, 2012). The work here suggests that the actual size of the virion itself may present an additional constraint particularly at mammalian body temperatures. Thus although the average diameter for HIV virions with a single core is 134 nm, individual virions display a broad range of diameters extending from 120 to 200 nm with a skewed distribution (Briggs *et al.*, 2003). Furthermore while the majority of HIV virions contained a single core, almost a third contained two or more cores. The mean diameter of the HIV virions containing a single core (134 ± 11 nm, $n = 89$) was significantly smaller than the mean diameter of virions containing two cores (158 ± 16 nm, $n = 43$) (Briggs *et al.*, 2003). Thus the magnitude of ΔS_{a_immob} may vary between individual HIV virions within the same exposure dose. The key conclusion from Fig. 5c is that the number of $CD4^+$ *T* cells with bound virus is highly sensitive to the magnitude of ΔS_{a_immob} with just a 4.5% increase in the magnitude of ΔS_{a_immob} from –290 to –277 J/mol/K for example increasing $C.V_T$ by five-fold from 1 to 5 $CD4^+$ *T* cells per mm^3 of blood at 37 °C. Thus smaller diameter viruses in a challenge does may have an advantage in binding and hence initiating infection at mammalian body temperatures. This also raises the question of the magnitude of ΔS_{a_immob} for an aggregate containing several virions of the same virus and in the case of EBOV, for the long filaments linking multiple genome copies (Beniac *et al.*, 2012). It has previously been proposed that fusing multiple genome copies into the same filament in the case of EBOV takes some of the entropy loss for ΔS_{a_immob} prior to binding to the cell surface (Gale 2017) such that aggregation can be viewed as a co-operative effect in the infection process. The effect of aggregation and virus size on the magnitude of ΔS_{a_immob} according to Eq. (18) needs to be investigated and understood to further the work here.

5. Conclusion

From a thermodynamic perspective, the affinity of virus binding to a host cell is greatly decreased at the higher body temperatures of mammals and birds such that temperature can be considered a constraint to be overcome. The relationship between binding affinity and temperature can be markedly affected by the change in heat capacity (ΔC_p) on virus binding through its effect on the enthalpy and entropy of the GP/Cr interaction. Specifically large negative values of ΔC_p reduce binding at both low and high temperatures giving a peak binding at a medium temperature as has been observed experimentally in binding of WEEV to mosquito midguts. Very large negative values of ΔC_p for protein/protein GP/Cr interactions are predicted to diminish arbovirus transmission at low temperatures compared to the HA/SA glycan interaction for which ΔC_p is negligible. Thus selecting for SA glycan interactions as reported for BTV binding may be a mechanism to allow transmission at the lower temperatures experienced by arboviruses infecting arthropods in temperate regions of the world.

The magnitude of ΔS_{a_immob} is currently unknown but is predicted to be large and negative and to be more negative for larger viruses such as HIV (mean diameter 134 nm) compared to the smaller arboviruses (diameter 50 to 70 nm). Small virion diameter through a less negative ΔS_{a_immob}, favours virus binding at higher temperatures giving smaller viruses a selective advantage for infecting hosts at the higher body temperatures of mammals and birds. This is in agreement with the published observational findings that virus volume decreases with increasing host temperature in the case of dsDNA viruses.

In the case of HIV, the unfavourable effect at human body temperature of the large negative ΔS_{a_immob} value due to the large size of the virus may be overcome by non-specific binding. It is proposed here that non-specific binding of HIV as the virus first randomly attaches to a host $CD4^+$ *T* cell surface takes a large proportion (represented by $\Delta S_{a\_non\_specific}$) of the entropy loss of ΔS_{a_immob} such that HIV can then bind specifically through Env:CD4 interactions at the relatively high temperature of the human body. The randomly attached virus "rolls into place" driven by $n = 3$ specific Env:CD4 interactions resulting in a further entropy loss ($\Delta S_{a\_specific}$) as the virus particle takes up a specific orientation ready for viral entry. Non-specific attachment factors are all the more important for a GP/Cr system such as the HIV Env:CD4 interaction for which ΔC_p is large and negative and diminishes binding at

higher temperatures.

It is concluded that experimental data on ΔS_{a_immob} should be obtained and antiviral therapeutic strategies, for example using zinc oxide nanoparticles for herpes simplex virus or neutralising antibodies to block virus binding, should focus not only on blocking the Cr-binding sites on the GP molecules themselves but also on targeting ΔS_{a_immob} by increasing the size of the virus itself and so minimising host cell binding affinity at human body temperatures according to the model here. Bacterial cells are larger than viruses and ΔS_{a_immob} would be expected to be more negative. Targeting ΔS_{a_immob} may also have application as an alternative approach to antibiotics for bacterial pathogens when bacterial pathogenesis depends on attachment to cells. However, it should be noted that ΔS_{a_immob} decreases logarithmically (i.e. slowly) with increasing size which may limit the practicability to bacteria.

Declaration of Competing Interest

None declared.

Acknowledgements

I thank the anonymous reviewer who helped me with the HIV binding data and greatly improved this manuscript.

Author Statement

I wrote the whole of this paper, did all the work and developed all the ideas. I have done this work in my spare time at home with no funding. I greatly enjoy doing this sort of paper.

Disclaimer

The views expressed in this paper are those of the author and not necessarily those of any organisations.

References

Antoine, T., Mishra, Y.K., Trigilio, J., Tiwari, V., Adelung, R., Shukla, D., 2012. Prophylactic, therapeutic and neutralizing effects of zinc oxide tetrapod structures against herpes simplex virus type-2 infection. Antiviral. Res. 96, 363–375.

Beniac, D.R., Melito, P.L., deVarennes, S.L., Hiebert, S., Rabb, M.J., Lamboo, L.L., Jones, S.M., Booth, T.F., 2012. The organisation of Ebola virus reveals a capacity for extensive modular polyploidy. PLoS ONE 7 (1), e29608.

Bennett, A.J., Bushmaker, T., Cameron, K., Ondzie, A., Niama, F.R., Parra, H.J., Mombouli, J.-V., Olson, S.H., Munster, V.J., Goldberg, T.L., 2018. Diverse rna viruses of arthropod origin in the blood of fruit bats suggest a link between bat and arthropod viromes. Virology 1, 64–72.

Brandenberg, O.F., Magnus, C., Rusert, P., Regoes, R.R., Trkola, A., 2015. Different infectivity of HIV-1 strains is linked to number of envelope trimers required for entry. PLoS Pathog. 11 (1), e1004595. https://doi.org/10.1371/journal.ppat.1004595.

Brault, A.C., 2009. Changing patterns of west Nile virus transmission: altered vector competence and host susceptibility. Vet. Res. 40, 43.

Briggs, J.A.G., Wilk, T., Welker, R., Krausslich, H.G., D.Fuller, Stephen, 2003. Structural organization of authentic, mature HIV-1 virions and cores. EMBO J. 22, 1707–1715.

Bull, R.A., Luciani, F., McElroy, K., Gaudieri, S., Pham, S.T., Chopra, A., Cameron, B., Maher, L., Dore, G.J., White, P.A., Lloyd, A.R., 2011. Sequential bottlenecks drive viral evolution in early acute hepatitis c virus infection. PLoS Pathog. 7, e1002243.

Bull, R.A., Eden, J.-S., Luciani, F., McElroy, K., Rawlinson, W.D., White, P.A., 2012. Contribution of intra- and interhost dynamics to norovirus evolution. J. Virol. 86, 3219–3229.

Carneiro, F.A., Bianconi, M.L., Weissmuller, G., Stauffer, F., Da Poian, A., 2002. Membrane recognition by vesicular stomatitis virus involves enthalphy-driven protein-lipid interactions. J. Virol. 76, 3756–3764.

Chuang, G.-Y., Geng, H., Pancera, M., Xu, K., Cheng, C., Acharya, P., Chambers, M., Druz, A., Tsybovsky, Y., Wanninger, T.G., Yang, Y., Doria-Rose, N.A., Georgiev, I.S., Gorman, J., Joyce, M.G., O'Dell, S., Zhou, T., McDermott, A.B., Mascola, J.R., Kwong, P.D., 2017. Structure-based design of a soluble prefusion-closed HIV-1 env trimer with reduced CD4 affinity and improved immunogenicity. J. Virol. 91 e02268-16.

Daszak, P., Zambrana-Torrelio, C., Bogicha, T.L., Fernandez, M., Epstein, J.H., Murray, K.A., Hamilton, H., 2013. Interdisciplinary approaches to understanding disease emergence: the past, present, and future drivers of Nipah virus emergence. Proc. Natl. Acad. Sci. USA 110 (Supplement 1), 3681–3688.

De Graaf, M., Fouchier, R.A.M., 2014. Role of receptor binding specificity in influenza a virus transmission and pathogenesis. EMBO J. 33, 823–841.

Dey, B., Pancera, M., Svehla, K., Shu, Y., Xiang, S.-H., Vainshtein, J., Li, Y., Sodroski, J., Kwong, P.D., Mascola, J.R., Wyatt, R., 2007. Characterization of human immunodeficiency virus type 1 monomeric and trimeric gp120 glycoproteins stabilized in the CD4-bound state: antigenicity, biophysics, and immunogenicity. J. Virol. 81, 5579–5593.

Dimitrov, D.S., Hillman, K., Manischewitz, J., Blumenthal, R., Golding, H., 1992. Kinetics of soluble CD4 binding to cells expressing human immunodeficiency virus type 1 envelope glycoprotein. J. Virol. 66, 132–138.

Doranz, B.J., Baik, S.S., Doms, R.W., 1999. Use of a gp120 binding assay to dissect the requirements and kinetics of human immunodeficiency virus fusion events. J. Virol. 73, 10346–10358.

Du, X., Li, Y., Xia, Y.-L., Ai, S.-M., Liang, J., Sang, P., Ji, X.-L., Liu, S.-Q., 2016. Insights into protein–ligand interactions: mechanisms, models, and methods. Int. J. Mol. Sci. 17, 144.

Erickson, A.M., Henry, B.I., Murray, J.M., Klasse, P.J., Angstmann, C.N., 2015. Predicting first traversal times for virions and nanoparticles in mucus with slowed diffusion. Biophys. J. 109, 164–172.

Fei, Y., Sun, Y.-S., Li, Y., Yu, H., Lau, K., Landry, J.P., Luo, Z., Baumgarth, N., Chen, X., Zhu, X., 2015. Characterization of receptor binding profiles of influenza a viruses using an ellipsometry-based label-free glycan microarray assay platform. Biomolecules 5 (1), 480–481 498.

Frey, S., Marsh, M., Günther, S., Pelchen-Matthews, A., Stephens, P., Ortlepp, S., Stegmann, T., 1995. Temperature dependence of cell-cell fusion induced by the envelope glycoprotein of human immunodeficiency virus type 1. J. Virol. 69, 1462–1472.

Gale, P., 2017. Could bat cell temperature and filovirus filament length explain the emergence of ebola virus in mammals? predictions of a thermodynamic model. Transbound. Emerg. Dis. 64, 1676–1693.

Gale, P., 2018. Using thermodynamic parameters to calibrate a mechanistic dose-response for infection of a host by a virus. Microbial Risk Anal. 8, 1–13.

Gale, P., 2019. Towards a thermodynamic mechanistic model for the effect of temperature on arthropod vector competence for transmission of arbovirus. Microbial Risk Anal. 12, 27–43.

Gupta, P., Mellors, J., Kingsley, L., Riddler, S., Singh, M.K., Schreiber, S., Cronin, M., Rinaldo, C.R., 1997. High viral load in semen of human immunodeficiency virus type 1-infected men at all stages of disease and its reduction by therapy with protease and nonnucleoside reverse transcriptase inhibitors. J. Virol. 71, 6271–6275.

Harada, S., Akaike, T., Yusa, K., Maeda, Y., 2004. Adsorption and infectivity of human immunodeficiency virus type 1 are modified by the fluidity of the plasma membrane for multiple-site binding. Microbiol. Immunol. 48 (4), 347–355.

Harrison, S.C., 2015. Viral membrane fusion. Virology 479-480, 498–507.

Hasan, S.S., Sun, C., Kim, A.S., Watanabe, Y., Chen, C.-L., Klose, T., Buda, G., Crispin, M., Diamond, M.S., Klimstra, W.B., Rossmann, M.G., 2018. Cryo-EM structures of eastern equine encephalitis virus reveal mechanisms of virus disassembly and antibody neutralization. Cell Rep. 25, 3136–3147.

Houk, E.J., Arcus, Y.M., Hardy, J.L., Kramer, L.D., 1990. Binding of western equine encephalomyelitis virus to brush border fragments isolated from mesenteronal epithelial cells of mosquitoes. Virus Res. 17, 105–117.

Huitron-Resendiz, S., Marcondes, M.C.G., Flynn, C.T., Lanigan, C.M.S., Fox, H.S., 2007. Effects of simian immunodeficiency virus on the circadian rhythms of body temperature and gross locomotor activity. Proc. Natl. Acad. Sci. USA 104, 15138–15143.

Jung, H.-I., Bowden, S.J., Cooper, A., Perham, R.N., 2002. Thermodynamic analysis of the binding of component enzymes in the assembly of the pyruvate dehydrogenase multienzyme complex of *Bacillus stearothermophilus*. Protein Sci. 11, 1091–1100.

Kinney, R.M., Huang, C.Y.H., Whiteman, M.C., Bowen, R.A., Langevin, S.A., Miller, B.R., Brault, A.C., 2006. Avian virulence and thermostable replication of the North American strain of west Nile virus. J. Gen. Virol. 87, 3611–3622.

Klasse, P.J., 2012. The molecular basis of HIV entry. Cell Microbiol. 14, 1183–1192.

Kuhmann, S.E., Platt, E.J., Kozak, S.L., Kabat, D., 2000. Cooperation of multiple CCR5 coreceptors is required for infections by human immunodeficiency virus type 1. J. Virol. 74, 7005–7015.

Leendertz, S.A.J., 2016. Testing new hypotheses regarding ebolavirus reservoirs. Viruses 8, 30.

Liu, Q., Acharya, P., Dolan, M.A., Zhang, P., Guzzo, C., Lu, J., Kwon, A., Gururani, D., Miao, H., Bylund, T., Chuang, G.-Y., Druz, A., Zhou, T., Rice, W.J., Wigge, C., Carragher, B., Potter, C.S., Kwong, P.D., Lusso, P., 2017a. Quaternary contact in the initial interaction of CD4 with the HIV-1 envelope trimer. Nat. Struct. Mol. Biol. 24, 370–378.

Liu, Z., Zhang, Z., Lai, Z., Zhou, T., Jia, Z., Gu, J., Wu, K., Chen, X.-G., 2017b. Temperature increase enhances *Aedes albopictus* competence to transmit Dengue virus. Front. Microbiol. 8, 2337.

Lu, G., Hu, Y., Wang, Q., Qi, J., Gao, F., Li, Y., Zhang, Y., Zhang, W., Yuan, Y., Bao, J., Zhang, B., Shi, Y., Yan, Y., Gao, G.F., 2013. Molecular basis of binding between novel human coronavirus MERS-COV and its cellular receptor CD26. Nature 500, 227–231.

Mammen, M., Choi, S.-K., Whitesides, G.M., 1998. Polyvalent interactions in biological systems: implications for design and use of multivalent ligands and inhibitors. Angew. Chem. Int. Ed. 37, 2754–2794.

Moore, J.P., Klasse, P.J., 1992. Thermodynamic and kinetic analysis of sCD4 binding to HIV-1 virions and of gp120 dissociation. AIDS Res. Hum. Retroviruses 8, 443–450.

Mukhopadhyay, S., Kim, B.S., Chipman, P.R., Rossmann, M.G., Kuhn, R.J., 2003. Structure of west Nile virus. Science 302, 248.

Mullens, B.A., Gerry, A.C., Lysyk, T.J., Schmidtmann, E.T., 2004. Environmental effects on vector competence and virogenesis of bluetongue virus in *Culicoides* interpreting laboratory data in a field context. Vet. Ital. 40, 160–166.

Myszka, D.G., Sweet, R.W., Hensley, P., Brigham-Burke, M., Kwong, P.D., Hendricksoni, W.A., Wyatt, R., Sodroski, J., Doyle, M.L., 2000. Energetics of the HIV gp120-CD4

binding reaction. Proc. Natl. Acad. Sci. USA 97, 9026–9031.
Nason, E.L., Rothagel, R., Mukherjee, S.K., Kar, A.K., Forzan, M., Prasad, B.V.V., Polly Roy, P., 2004. Interactions between the inner and outer capsids of bluetongue virus. J. Virol. 78, 8059–8067.
Ngai, K.L.K., Chan, M.C.W., Chan, P.K.S., 2013. Replication and transcription activities of ribonucleoprotein complexes reconstituted from avian H5N1, H1N1pdm09 and H3N2 influenza A viruses. PLoS ONE 8 (6), e65038. https://doi.org/10.1371/journal.pone.0065038.
Nifong, R.L., Gillooly, J.F., 2016. Temperature effects on virion volume and genome length in dsDNA viruses. Biol. Lett. 12, 20160023.
O'Shea, T.J., Ctyan, P.M., Cunnignham, A.A., Fooks, A.R., Hayman, D.T.S., Luis, A.D., Peel, A.J., Plowright, R.K, Wood, J.L.N., 2014. Bat flight and zoonotic viruses. Emerg. Infect. Dis. 20, 741–745.
Saez, A.M., Weiss, S., Nowak, K., Lapeyre, V., Zimmermann, F., Dux, A., Kuhl, H.S., Kaba, M., et al., 2015. Investigating the zoonotic origin of the west African Ebola epidemic. EMBO Mol. Med. 7, 17–23.
Sharp, P.M., Shaw, G.M., Hahn, B.H., 2005. Simian immunodeficiency virus infection of Chimpanzees. J. Virol. 79, 3891–3902.
Thakar, M.R., Abraham, P.R., Arora, S., Balakrishnan, P., Bandyopadhyay, B., Joshi, A.A., Devi, K.R., Vasanthapuram, R., Vajpayee, M., Desai, A., Mohanakrishnan, J., Narain, K., Ray, K., Patil, S.S., Singh, R., Singla, A., Paranjape, R.S., 2011. Establishment of reference CD4+ t cell values for adult Indian population. AIDS Res. Ther. 8, 35.
Wilen, C.B., Tilton, J.C., Doms, R.W., 2012. HIV: cell binding and entry. in additional perspectives on HIV. In: Bushman, Frederic D., Nabel, Gary J., Swanstrom, Ronald (Eds.), Cold Spring Harbor Perspectives in Medicine 2012, a006866.
Xiong, X., Coombs, P.J., Martin, S.R., Liu, J., Xiao, H., McCauley, J.W., Locher, K., Walker, P.A., Collins, P.J., Kawaoka, Y., Skehel, J.J., Gamblin, S.J., 2013. Receptor binding by a ferret-transmissible H5 avian influenza. Nature 497, 392–396.
Xu, K., Chan, Y.-.P., Rajashankar, K.R., Khetawat, D., Yan, L., Momchil, V., Kolev, M.V., Broder, C.C., Nikolov, D.B., 2012. New insights into the Hendra virus attachment and entry process from structures of the virus G glycoprotein and its complex with ephrin-B2. PLoS ONE 7, e48742.
Yang, X., Kurteva, S., Ren, X., Lee, S., Sodroski, J., 2005. Stoichiometry of envelope glycoprotein trimers in the entry of human immunodeficiency virus type 1. J. Virol. 79, 12132–12147.
Yuan, S., Cao, L., Ling, H., Dang, M., Sun, Y., Zhang, X., Chen, Y., Zhang, L., Su, D., Wang, X., Rao, Z., 2015. TIM-1 acts a dual-attachment receptor for Ebolavirus by interacting directly with viral GP and the PS on the viral envelope. Protein Cell 6 (11), 814–824.
Zhang, X., Boyce, M., Bhattacharya, B., Zhang, X., Schein, S., Roy, P., Zhou, Z.H., 2010. Bluetongue virus coat protein VP2 contains sialic acid-binding domains, and VP5 resembles enveloped virus fusion proteins. PNAS 107, 6292–6297.